Table 1. Limb Abnormalities in *Smoc1*$^{Tp/Tp}$ Mutants

Genotype	Talipes Valgus (No. of Affected/ Total No. of Pups)	Forelimb Abnormalities (No. of Limbs)	Hindlimb Syndactyly (No. of Limbs)					Other External Abnormalities (No. of Pups)	4th and 5th Metatarsal Fusion (No. of Affected/Total No. of Limbs)
			None	2/3[a]	3/4[b]	2/3/4[c]	4 Digits		
Postnatal Day 0									
Smoc1$^{Tp/+}$ (line 1, C57BL/6J)	0/42	0	84	0	0	0	0		
Smoc1$^{Tp/+}$ (line 2, ICR mixed)	0/38	0	76	0	0	0	0		
Smoc1$^{Tp/Tp}$ (line 1, C57BL/6J)	10/10	0	3	0	3	12	2		
Smoc1$^{Tp/Tp}$ (line 2, ICR mixed)	13/17	1[d]	1	1	9	4	19	cleft palate (3)	
Postnatal Day 14									
Smoc1$^{Tp/+}$ (line 1, C57BL/6J)	0/70	0	140	0	0	0	0		
Smoc1$^{Tp/Tp}$ (line 1, C57BL/6J)	11/11	18[e]	2	7	3	8	2	hypoplastic thumbs (5)	9/10[f]

[a] Syndactyly between the 2nd and 3rd digits.
[b] Syndactyly between the 3rd and 4th digits.
[c] Syndactyly between the 2nd, 3rd, and 4th digits.
[d] 2/3 soft tissue syndactyly.
[e] Eleven limbs showed 2/3 webbing, four limbs showed 2/3 soft tissue syndactyly, and one limb showed 3/4 syndactyly.
[f] Based on examination of skeletal preparations.

probe; Tomonori Hirose, Kazunori Akimoto, and Kazunori Sasaki (Yokohama City University) for providing useful information about mouse breeding, taking photos on a stereo microscope, and mRNA quantification; and Kohei Shiota and Sumiko Kimura (Kyoto University) for helpful comments about NB staining and limb anomalies. This work was supported by research grants from the Ministry of Health, Labour and Welfare (T. Furuichi, N. Miyake, N. Matsumoto, and H.S.) and the Japan Science and Technology Agency (N. Matsumoto), a Grant-in-Aid for Scientific Research from the Japan Society for the Promotion of Science (T. Furuichi and N. Matsumoto), and a Grant-in-Aid for Young Scientist from the Japan Society for the Promotion of Science (K.N., H.D., N. Miyake, and H.S.). This work has been carried out at the Advanced Medical Research Center of Yokohama City University.

Received: September 29, 2010
Revised: November 20, 2010
Accepted: November 26, 2010
Published online: December 30, 2010

Web Resources

The URLs for data presented herein are as follows:

BDGP, http://www.fruitfly.org/
ESEfinder 3.0, http://rulai.cshl.edu/cgi-bin/tools/ESE3/esefinder.cgi?process=home
GenBank, http://www.ncbi.nlm.nih.gov/Genbank/
HSF2.4.1, http://www.umd.be/HSF/
NetGene2, http://www.cbs.dtu.dk/services/NetGene2/
Online Mendelian Inheritance in Man, http://www.ncbi.nlm.nih.gov/Omim
UCSC Genome Browser, http://genome.ucsc.edu/cgi-bin/hgGateway
SpliceView, http://zeus2.itb.cnr.it/~webgene/wwwspliceview.html

References

1. Waardenburg, P.J. (1961). Autosomally-recessive anophthalmia with malformations of the hands and feet. In Genetics and Ophthalmology, P.J. Waardenburg, A. Franceschetti, and D. Klein, eds. (Assen, The Netherlands: Royal Van Gorcum), p. 773.
2. Teiber, M.L., Garrido, J.A., and Barreiro, C.Z. (2007). Ophthalmo-acromelic syndrome: report of a case with vertebral anomalies. Am. J. Med. Genet. A. *143A*, 2460–2462.
3. Garavelli, L., Pedori, S., Dal Zotto, R., Franchi, F., Marinelli, M., Croci, G.F., Bellato, S., Ammenti, A., Virdis, R., Banchini, G., and Superti-Furga, A. (2006). Anophthalmos with limb anomalies (Waardenburg opththalmo-acromelic syndrome): report of a new Italian case with renal anomaly and review. Genet. Couns. *17*, 449–455.
4. Tekin, M., Tutar, E., Arsan, S., Atay, G., and Bodurtha, J. (2000). Ophthalmo-acromelic syndrome: report and review. Am. J. Med. Genet. *90*, 150–154.
5. Adler, R., and Canto-Soler, M.V. (2007). Molecular mechanisms of optic vesicle development: complexities, ambiguities and controversies. Dev. Biol. *305*, 1–13.
6. Zeller, R., López-Ríos, J., and Zuniga, A. (2009). Vertebrate limb bud development: moving towards integrative analysis of organogenesis. Nat. Rev. Genet. *10*, 845–858.
7. Bakrania, P., Efthymiou, M., Klein, J.C., Salt, A., Bunyan, D.J., Wyatt, A., Ponting, C.P., Martin, A., Williams, S., Lindley, V., et al. (2008). Mutations in BMP4 cause eye, brain, and digit

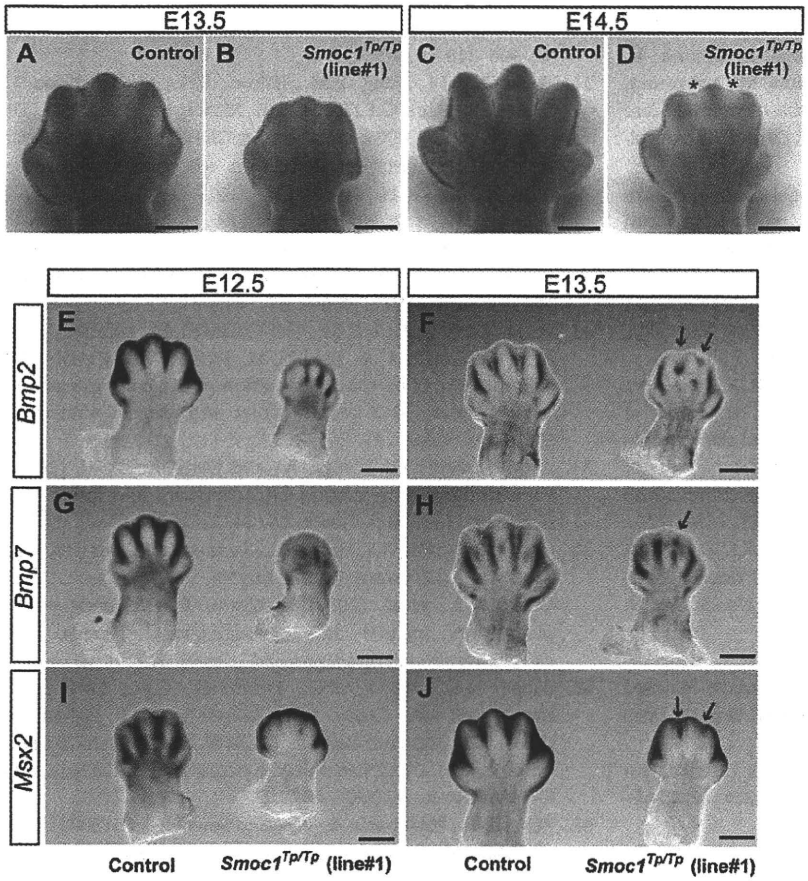

Figure 5. Reduced Apoptosis and Altered BMP Signaling in the Interdigital Mesenchyme of *Smoc1* Null Mice

(A–D) NB staining of left hindlimbs at E13.5 (A and B) and E14.5 (C and D). In comparison to control embryos (WT and $Smoc1^{Tp/+}$ littermates) (A and C), the number of NB-stained apoptotic cells in the interdigital mesenchyme of $Smoc1^{Tp/Tp}$ mice was dramatically reduced between digits 2 and 3 and digits 3 and 4 at both E13.5 and E14.5, and the webbing remained at a distal level (B and D, magenta asterisk).

(E–J) Whole-mount in situ hybridization of right hindlimbs at E12.5 (E, G, and I) and E13.5 (F, H, and J). At E12.5, interdigital expression of *Bmp2*, *Bmp7*, and *Msx2* was profoundly delayed in the hindlimbs of $Smoc1^{Tp/Tp}$ mice, and their expression in the interdigital mesenchyme was apparently perturbed, even at E13.5 (magenta arrows). Scale bar represents 500 μm.

developmental anomalies: overlap between the BMP4 and hedgehog signaling pathways. Am. J. Hum. Genet. *82*, 304–319.

8. Bornstein, P., and Sage, E.H. (2002). Matricellular proteins: extracellular modulators of cell function. Curr. Opin. Cell Biol. *14*, 608–616.
9. Vannahme, C., Smyth, N., Miosge, N., Gösling, S., Frie, C., Paulsson, M., Maurer, P., and Hartmann, U. (2002). Characterization of SMOC-1, a novel modular calcium-binding protein in basement membranes. J. Biol. Chem. *277*, 37977–37986.
10. Gersdorff, N., Müller, M., Schall, A., and Miosge, N. (2006). Secreted modular calcium-binding protein-1 localization during mouse embryogenesis. Histochem. Cell Biol. *126*, 705–712.
11. Thomas, J.T., Canelos, P., Luyten, F.P., and Moos, M., Jr. (2009). Xenopus SMOC-1 inhibits BMP signaling downstream of receptor binding and is essential for post-gastrulation development in Xenopus. J. Biol. Chem. *284*, 18994–19005.
12. Hamanoue, H., Megarbane, A., Tohma, T., Nishimura, A., Mizuguchi, T., Saitsu, H., Sakai, H., Miura, S., Toda, T., Miyake, N., et al. (2009). A locus for ophthalmo-acromelic syndrome mapped to 10p11.23. Am. J. Med. Genet. A. *149A*, 336–342.
13. Mégarbané, A., Souraty, N., and Tamraz, J. (1998). Ophthalmo-acromelic syndrome (Waardenburg) with split hand and polydactyly. Genet. Couns. *9*, 195–199.
14. Cogulu, O., Ozkinay, F., Gündüz, C., Sapmaz, G., and Ozkinay, C. (2000). Waardenburg anophthalmia syndrome: report and review. Am. J. Med. Genet. *90*, 173–174.
15. Miyake, N., Kosho, T., Mizumoto, S., Furuichi, T., Hatamochi, A., Nagashima, Y., Arai, E., Takahashi, K., Kawamura, R., Wakui, K., et al. (2010). Loss-of-function mutations of CHST14 in a new type of Ehlers-Danlos syndrome. Hum. Mutat. *31*, 966–974.
16. Gudbjartsson, D.F., Thorvaldsson, T., Kong, A., Gunnarsson, G., and Ingolfsdottir, A. (2005). Allegro version 2. Nat. Genet. *37*, 1015–1016.
17. Keng, V.W., Yae, K., Hayakawa, T., Mizuno, S., Uno, Y., Yusa, K., Kokubu, C., Kinoshita, T., Akagi, K., Jenkins, N.A., et al. (2005). Region-specific saturation germline mutagenesis in mice using the Sleeping Beauty transposon system. Nat. Methods *2*, 763–769.
18. Mamo, S., Gal, A.B., Bodo, S., and Dinnyes, A. (2007). Quantitative evaluation and selection of reference genes in mouse oocytes and embryos cultured in vivo and in vitro. BMC Dev. Biol. *7*, 14.
19. Parr, B.A., Shea, M.J., Vassileva, G., and McMahon, A.P. (1993). Mouse Wnt genes exhibit discrete domains of expression in the early embryonic CNS and limb buds. Development *119*, 247–261.
20. Saitsu, H., Ishibashi, M., Nakano, H., and Shiota, K. (2003). Spatial and temporal expression of folate-binding protein 1 (Fbp1) is closely associated with anterior neural tube closure in mice. Dev. Dyn. *226*, 112–117.
21. Tamplin, O.J., Kinzel, D., Cox, B.J., Bell, C.E., Rossant, J., and Lickert, H. (2008). Microarray analysis of Foxa2 mutant mouse embryos reveals novel gene expression and inductive roles

for the gastrula organizer and its derivatives. BMC Genomics *9*, 511.

22. Suzuki, D., Yamada, A., Amano, T., Yasuhara, R., Kimura, A., Sakahara, M., Tsumaki, N., Takeda, S., Tamura, M., Nakamura, M., et al. (2009). Essential mesenchymal role of small GTPase Rac1 in interdigital programmed cell death during limb development. Dev. Biol. *335*, 396–406.
23. Kimura, S., and Shiota, K. (1996). Sequential changes of programmed cell death in developing fetal mouse limbs and its possible roles in limb morphogenesis. J. Morphol. *229*, 337–346.
24. Sernagor, E., Eglen, S.J., and Wong, R.O. (2001). Development of retinal ganglion cell structure and function. Prog. Retin. Eye Res. *20*, 139–174.
25. Bandyopadhyay, A., Tsuji, K., Cox, K., Harfe, B.D., Rosen, V., and Tabin, C.J. (2006). Genetic analysis of the roles of BMP2, BMP4, and BMP7 in limb patterning and skeletogenesis. PLoS Genet. *2*, e216.
26. Robert, B. (2007). Bone morphogenetic protein signaling in limb outgrowth and patterning. Dev. Growth Differ. *49*, 455–468.
27. Dudley, A.T., Lyons, K.M., and Robertson, E.J. (1995). A requirement for bone morphogenetic protein-7 during development of the mammalian kidney and eye. Genes Dev. *9*, 2795–2807.
28. Khokha, M.K., Hsu, D., Brunet, L.J., Dionne, M.S., and Harland, R.M. (2003). Gremlin is the BMP antagonist required for maintenance of Shh and Fgf signals during limb patterning. Nat. Genet. *34*, 303–307.
29. Furuta, Y., and Hogan, B.L. (1998). BMP4 is essential for lens induction in the mouse embryo. Genes Dev. *12*, 3764–3775.
30. Asai-Coakwell, M., French, C.R., Berry, K.M., Ye, M., Koss, R., Somerville, M., Mueller, R., van Heyningen, V., Waskiewicz, A.J., and Lehmann, O.J. (2007). GDF6, a novel locus for a spectrum of ocular developmental anomalies. Am. J. Hum. Genet. *80*, 306–315.
31. Tassabehji, M., Fang, Z.M., Hilton, E.N., McGaughran, J., Zhao, Z., de Bock, C.E., Howard, E., Malass, M., Donnai, D., Diwan, A., et al. (2008). Mutations in GDF6 are associated with vertebral segmentation defects in Klippel-Feil syndrome. Hum. Mutat. *29*, 1017–1027.
32. Wyatt, A.W., Osborne, R.J., Stewart, H., and Ragge, N.K. (2010). Bone morphogenetic protein 7 (BMP7) mutations are associated with variable ocular, brain, ear, palate, and skeletal anomalies. Hum. Mutat. *31*, 781–787.
33. Ye, M., Berry-Wynne, K.M., Asai-Coakwell, M., Sundaresan, P., Footz, T., French, C.R., Abitbol, M., Fleisch, V.C., Corbett, N., Allison, W.T., et al. (2010). Mutation of the bone morphogenetic protein GDF3 causes ocular and skeletal anomalies. Hum. Mol. Genet. *19*, 287–298.
34. Zhou, F., Leder, P., Zuniga, A., and Dettenhofer, M. (2009). Formin1 disruption confers oligodactylism and alters Bmp signaling. Hum. Mol. Genet. *18*, 2472–2482.
35. Chang, B., Smith, R.S., Peters, M., Savinova, O.V., Hawes, N.L., Zabaleta, A., Nusinowitz, S., Martin, J.E., Davisson, M.L., Cepko, C.L., et al. (2001). Haploinsufficient Bmp4 ocular phenotypes include anterior segment dysgenesis with elevated intraocular pressure. BMC Genet. *2*, 18.
36. Ragge, N.K., Brown, A.G., Poloschek, C.M., Lorenz, B., Henderson, R.A., Clarke, M.P., Russell-Eggitt, I., Fielder, A., Gerrelli, D., Martinez-Barbera, J.P., et al. (2005). Heterozygous mutations of OTX2 cause severe ocular malformations. Am. J. Hum. Genet. *76*, 1008–1022.
37. Behesti, H., Papaioannou, V.E., and Sowden, J.C. (2009). Loss of Tbx2 delays optic vesicle invagination leading to small optic cups. Dev. Biol. *333*, 360–372.

Epilepsia, 51(9):1679–1684, 2010
doi: 10.1111/j.1528-1167.2010.02559.x

FULL-LENGTH ORIGINAL RESEARCH

Frameshift mutations of the *ARX* gene in familial Ohtahara syndrome

***Mitushiro Kato, †Norihisa Koyama, ‡Masayasu Ohta, §Kiyokuni Miura, and *Kiyoshi Hayasaka**

***Department of Pediatrics, Yamagata University Faculty of Medicine, Yamagata, Japan; †Department of Pediatrics, Toyohashi Municipal Hospital, Toyohashi, Japan; ‡Department of Pediatrics, Toride Kyodo General Hospital, Toride, Japan; and §Department of Pediatrics, Toyota Municipal Child Development Center, Toyota, Japan**

Summary

Purpose: Ohtahara syndrome is one of the most severe and earliest forms of epilepsy and is frequently associated with brain malformations, such as hemimegalencephaly. Recently, longer expansion of the first polyalanine tract of *ARX* was found to be causative for Ohtahara syndrome without brain malformation, whereas premature termination mutations of *ARX* were found to cause severe brain malformations, such as lissencephaly or hydranencephaly. Both are designated as *ARX*-related interneuronopathies.

Methods: We investigated the molecular basis of Ohtahara syndrome in two families, comprising six male patients in two generations demonstrating X-linked inheritance.

Results: Novel frameshift mutations in the terminal exon of the *ARX* gene (Ala524fsX534 and E536fsX672) were identified in two patients (2 and 13 years, each) from both families. Two patients developed West syndrome, and one of these later developed Lennox-Gastaut syndrome. Brain magnetic resonance imaging (MRI) of all patients showed no brain malformations in contrast to the patients with a premature termination mutation in other exons of *ARX*.

Discussion: The etiology of Ohtahara syndrome is heterogeneous; however, the molecular analysis of *ARX* should be considered in sporadic or familial male patients with Ohtahara syndrome.

KEY WORDS: Epileptic encephalopathy, Interneuron, Nonsense-mediated mRNA decay, West syndrome, Lennox-Gastaut syndrome.

Ohtahara syndrome, or early infantile epileptic encephalopathy with suppression-burst, is one of the most severe and earliest forms of epilepsy. The onset of the initial seizure usually occurs during the neonatal period, and most patients with Ohtahara syndrome show severe developmental delay (Yamatogi & Ohtahara, 2002). Tonic spasms are the main seizure type and frequently occur every day. This is shown on an electroencephalography (EEG) as an initial suppression-burst pattern that shifts to hypsarrhythmia, leading to West syndrome several months after onset. Ohtahara syndrome is classified as a symptomatic epileptic syndrome and was believed to be noninherited in most cases because of its frequent association with hemimegalencephaly or other brain malformations (Commission on Classification and Terminology of the International League Against Epilepsy, 1989).

Recently, two genes, *ARX* and *STXBP1*, have been found to be responsible for Ohtahara syndrome (Kato et al., 2007; Saitsu et al., 2008). *ARX* (*aristaless*-related homeobox) consists of five exons encoding a 562 amino acid protein (Kitamura et al., 2002). The ARX protein has four polyalanine tracts, in which 7–16 alanine residues are sequentially repeated. The *ARX* gene is located on human chromosome Xp22.13 and is expressed in γ-aminobutyric acid (GABA)ergic interneurons in the fetal brain. Mutations of *ARX* cause a wide variety of X-linked phenotypes, such as nonsyndromic mental retardation, Partington syndrome, West syndrome, Proud syndrome, and X-linked lissencephaly with abnormal genitalia (Gecz et al., 2006; Kato et al., 2004). There is a strong correlation between genotype and phenotype (Kato et al., 2004). Premature termination or null mutations cause brain malformations, such as lissencephaly, hydranencephaly, and agenesis of the corpus callosum, whereas expansion of polyalanine tracts gives rise to non-malformation groups, such as mental retardation, dystonia, and epilepsy including West syndrome and Ohtahara syndrome. The expansion length of Ohtahara syndrome (33-bp) is longer than that of patients with nonsyndromic mental retardation (6 or 9-bp) or West syndrome with dystonia (21-bp) (Guerrini et al., 2007), and the length of the first polyalanine tract is correlated with the severity and onset of diseases (Kato et al., 2007). Patients with Ohtahara

Accepted February 5, 2010; Early View publication April 2, 2010.
Address correspondence to Mitushiro Kato, Department of Pediatrics, Yamagata University Faculty of Medicine, 2-2-2, Iida-nishi, Yamagata 990-9585, Japan. E-mail: mkato@med.id.yamagata-u.ac.jp

syndrome caused by polyalanine expansion of *ARX* show similar findings and clinical courses, such as hypoplastic external genitalia or progressive atrophy of the cerebrum, in addition to the OS phenotype (Kato et al., 2007). Interestingly, deletion of exon 5 was reported in a small family with severe West syndrome without brain malformation (Stromme et al., 2002), and the size of truncated mRNA was found to be unrelated to the severity of brain malformations if the mutations are in exons 1–4 (Kato et al., 2004), suggesting the involvement of nonsense-mediated mRNA decay in the pathogenesis of *ARX*-related diseases.

In this report, we show that frameshift mutations in exon 5 of *ARX* are also causative for two pedigrees involving Ohtahara syndrome and other epileptic encephalopathies without brain malformations.

Clinical Findings

In Family 1 (Fig. 1A), Patient 1 (III-2) was the second child of unrelated healthy Japanese parents. He had two sisters by two different fathers, and his elder sister had a developmental speech delay and growth hormone–deficient short statue, 97.9 cm [−2.6 standard deviation (SD)] at 5 years and 6 months. His mother had a healthy younger sister and two affected elder brothers (II-1 and 2) with similar histories and conditions, such as convulsions, dystonic posture, and profound psychomotor delay in addition to being bed-ridden, who died in infancy. Patient 1 was born at 42 weeks of gestation by spontaneous vaginal delivery after an uneventful pregnancy. His birth weight was 2,798 g (−1.0 SD), his height was 48.0 cm (−0.9 SD), and his head circumference was 30.5 cm (−2.1 SD). At the age of 1 month, he was diagnosed with Ohtahara syndrome after he presented with tonic spasms, which sometimes occurred in clusters associated with a suppression-burst pattern on EEG (Fig. 2A). The EEG finding evolved to hypsarrhythmia (Fig. 2B) from 3 months of age, which was compatible with West syndrome. He was treated frequently with mechanical ventilation due to recurrent aspiration pneumonia until a tracheal separation procedure was performed as part of a tracheostomy at the age of 29 months. He unexpectedly showed dystonic posture from 27 months. At the age of 28 months, his height was 84.8 cm (−0.9 SD), his weight was 8,070 g (−3.1 SD), and his head circumference was 44.1 cm (−3.1 SD). He had severe scoliosis, mild undescended testes with a normal penis, severe spastic quadriplegia, profound mental retardation, and generalized tonic seizures with upward eye gazing lasting several seconds frequently each day. Treatments with pyridoxal phosphate, valproic acid, benzodiazepines including clonazepam, barbiturates including phenobarbital, and zonisamide were ineffective. Topiramate showed partial effectiveness against his seizures from 34 months of age, but his EEG still showed a suppression-burst pattern during sleep state (Fig. 2C,D). Blood tests showed elevation of liver transaminase [aspartate aminotransferase (AST) 147 IU/L, alanine aminotransferase (ALT) 101 IU/L, lactate dehydrogenase (LDH) 414 IU/L], hyponatremia (Na 129 mEq/L), and myoglobinemia [myoglobin 215 ng/ml, creatine kinase (CK) 647 IU/L] associated with severe pneumonia. His chromosome arrangement was 46,XY. His brain MRI was normal in early infancy, but then showed slightly progressive ventricular dilation and cortical atrophy. His basal ganglia demonstrated a slightly high spotted signal at 33 months of age. His scoliosis began improving at 35 months.

In Family 2 (Fig. 1B), Patient 2 (III-2) was the second son of a healthy mother. The pregnancy was uneventful, and delivery occurred at term without asphyxia. His birth weight was 2,968 g, and his head circumference was 32 cm. Tonic spasms involving flexion of the neck and extremities started from 22 days of age and occurred in clusters. An interictal EEG at 43 days showed a suppression-burst pattern (Fig. S1A,B). An ictal video-EEG demonstrated two different patterns, a high-amplitude slow wave combined with tonic spasms and a diffuse irregular polyspike-and-wave (Fig. S1C) with generalized myoclonic seizures or upward eye gazing. His brain MRI at 47 days of age was normal. High doses of pyridoxine and thyrotropin-releasing hormone (TRH) injection were ineffective, and valproic acid could not be administered because of vomiting. At the age of 2 months, his seizures temporarily disappeared after 3 days of adrenocorticotropic hormone (ACTH) injection (0.01 mg/kg/day). At the age of 3 months, he started to have hypokinetic seizures with oral automatism and cyanosis lasting 1 min, which were similar to complex partial seizures, and secondary generalized tonic–clonic seizures lasting 1–3 min that occurred several times a month and were treated with carbamazepine (Fig. S1D). Myoclonus and spasms appeared from the age of 5 months, which were controlled by clonazepam after 8 months. No epileptic discharges were shown on waking EEG from the age of 6 months. He remained seizure free from the age of

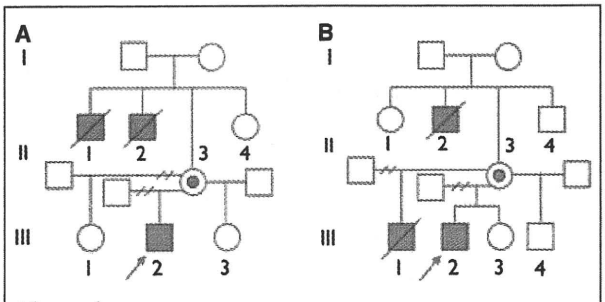

Figure 1.
Pedigrees of family 1 (**A**) and family 2 (**B**). The probands are indicated by an orange arrow. Green solid symbols denote affected individuals, and dotted circles denote asymptomatic obligatory female carriers. Open symbols denote unaffected individuals.

Epilepsia, 51(9):1679–1684, 2010
doi: 10.1111/j.1528-1167.2010.02559.x

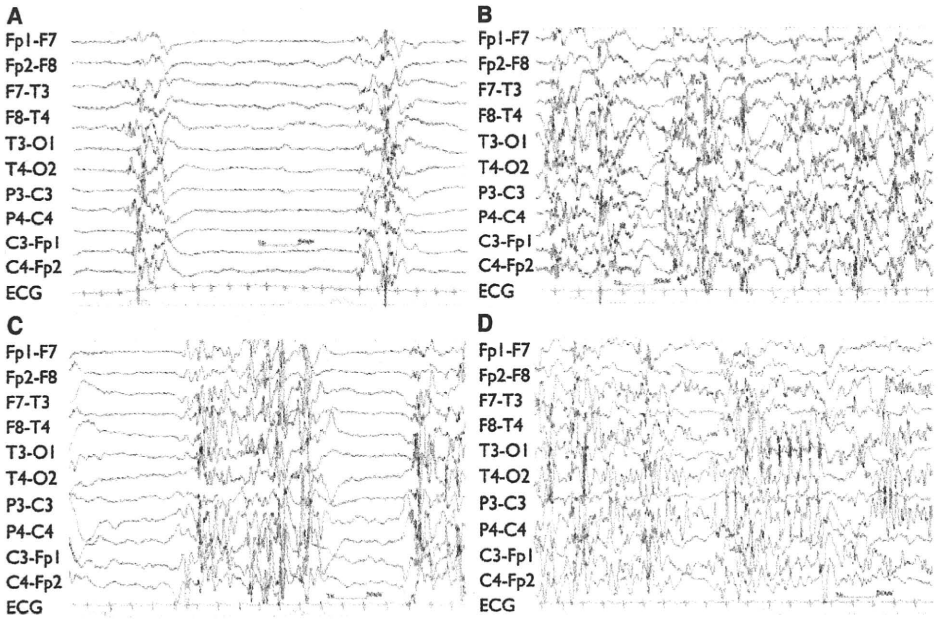

Figure 2.
Interictal electroencephalography (EEG) of Patient 1. The suppression-burst pattern comprised flattening of background activity and an intermittent irregular polyspike and slow wave bursts at 1 month (**A**) changed to hypsarrhythmia with an irregularly continuous slow wave with multifocal or diffuse paroxysmal discharges in the awake state (**B**). At 34 months, the suppression-burst pattern was observed only when the patient was asleep (**C**), but left dominant hemispheric spike-and-slow wave or fast waves were seen in the awake state (**D**).

29–44 months, with an increased dose of carbamazepine and diazepam for muscular hypertonus. Tonic seizures with cyanosis lasting 30–60 s arose at 45 months of age. At the age of 13 years, he showed marked growth failure (height 108 cm, weight 11.6 kg); microcephaly (47 cm, −5.1 SD); severe spastic quadriplegia with no voluntary movements; myoclonic seizures or tonic seizures, which occurred as a single seizure or as clusters of seizures 10–20 times a day; no social contact; and no reaction to optic or acoustic stimuli. His external genitalia showed a relatively small penis (40 mm in length) and testes (1 ml in volume) because of delayed puberty. An EEG at the age of 2 years showed infrequent spikes during sleep state. A brain MRI at the age of 46 months demonstrated mild dilation of the lateral ventricles without worsening compared to that at the age of 13 years. All tests for metabolic disorders and prenatal infections were normal except for high blood and cerebrospinal fluid levels of lactate (26.9 and 24.6 mg/dl, respectively) and pyruvate (1.08 and 1.70 mg/dl, respectively) in early infancy. Chromosomal analysis revealed a pericentric inversion of chromosome 9, 46,XY, inv(9)(p11q13), which was supposed to be a normal variant based on the public databases (Starke et al., 2002).

Patient 3 (Fig. 1B, III-1) was the elder half-brother of Patient 2. He was spontaneously born at term without asphyxia. He started to have tonic spasms in flexion associated with irregular diffuse polyspikes and wave bursts with multifocal spikes on interictal sleep EEG from 3 weeks of age. The spasms were increasingly grouped in clusters. His sleep EEG demonstrated a suppression-burst pattern compatible with Ohtahara syndrome from 46 days to 3 months and then changed to show hypsarrhythmia compatible with West syndrome from 4 months. Treatment with valproic acid and clonazepam reduced the seizure frequency until 8 months, and then the clusters of tonic spasms worsened. At the age of 11 months, administration of ACTH (0.015 mg/kg/day) stopped his seizures after 10 days, but hypsarrhythmia was still observed on EEG, and solitary spasms reappeared despite a second course of ACTH therapy (0.02 mg/kg/day) at 13 months. At the age of 27 months, he demonstrated several types of generalized seizures, such as myoclonic seizures and tonic seizures when awake, brief tonic seizures in clusters during sleep, and clonic seizures provoked by high fever. His EEG showed frequent multifocal or diffuse paroxysmal discharges. A brain MRI at 35 months demonstrated microcephaly. At the age of 6 years and 2 months, he had tonic–clonic convulsions—sometimes followed by brief tonic seizures that occurred in clusters and were associated with bursts of diffuse slow spike-waves during both sleep

and wakefulness—which were compatible with Lennox-Gastaut syndrome. He showed microcephaly (46 cm, −3.8 SD), profound mental retardation with no social contact, and severe motor disturbance with no head control at the time of his death of gastroenteritis-related dehydration at the age of 6 years and 7 months. Blood and urine tests including metabolic disorders and prenatal infections were normal. A G-band chromosome test showed 46,XY.

Patient 4 (Fig. 1B, II-2) was the elder brother of the mother of Patients 2 and 3. He showed tonic spasms that occurred in clusters associated with abnormal EEG 2 months after birth. His seizures disappeared after treatment with AEDs, but he had cerebral palsy and died of recurrent pneumonia at the age of 8 months.

Methods

Blood samples were collected from two patients (Patients 1 and 2) and from their mother, after informed consent from the guardians and approval from the Yamagata University School of Medicine Institutional Review Board had been obtained. Genomic DNA was extracted according to standard procedures and was amplified for all coding exons and flanking introns of *ARX*. The primers and polymerase chain reaction (PCR) conditions have been described elsewhere (Kato et al., 2004). Bidirectional direct sequencing of the purified PCR products was performed on an automated DNA sequencer [ABI 310 (Applied Biosystems, Foster City, CA, U.S.A.].

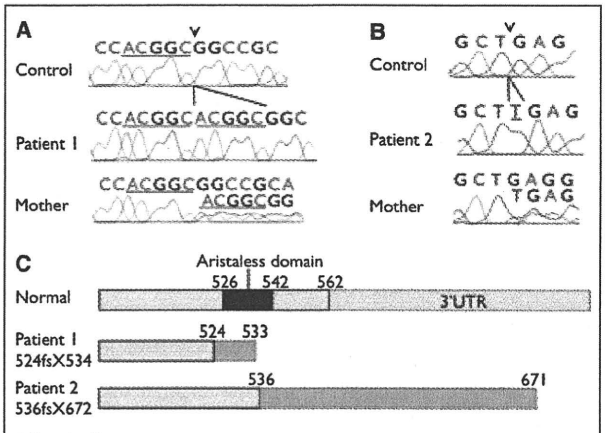

Figure 3.
Electropherograms of Family 1 (**A**) and Family 2 (**B**). Both patients carry hemizygous mutant sequences (**A**, 1564_1568dupACGGC; **B**, 1604_1605insT) and both mothers have heterozygous mutant and wild type sequences. Predicted protein length translated from the mutant exon 5 of *ARX* is truncated in Patient 1 and is elongated in Patient 2 compared to that of the wild type (**C**). The numbers on the bar represent the position of each amino acid residue starting from the first methionine. The green bars depict abnormally translated amino acids. UTR, untranslated region.

Results

Both families carried two different novel frameshift mutations in exon 5 of the *ARX* gene (Fig. 3). Patient 1 had a hemizygous 5 base pair (bp) duplication (1564_1568dupACGGC), resulting in a truncated protein with 523 N-terminal amino acids containing 10 abnormal amino acid residues (A524fsX534). The mother of Patient 1 had the same mutation heterozygously. Patient 2 had a hemizygous 1-bp insertion (1604_1605insT), which was thought to result in a frameshift from glutamate at amino acid 536 and alter the position of a stop codon in the 3′ UTR (untranslated region) leading to 138 abnormally elongated amino acid residues (E536fsX672). Patient 2 also carried a 9-bp deletion in exon 2 (325_333delGCGGCGGCG), resulting in a contraction of the first polyalanine tract from its original length of 16 alanine residues to 13 alanine residues. The mother of Patient 2 carried both changes heterozygously. None of these mutations identified in our patients were found in the 200 male and 100 female controls (400 X chromosomes).

Discussion

We report two families with Ohtahara syndrome showing characteristic clinical features, such as early onset tonic spasms with suppression-burst patterns on EEG, evolution to West syndrome, and severe developmental delay. Although familial West syndrome or infantile spasms have been reported in a number of articles (Kato, 2006), familial Ohtahara syndrome is rare, and a case involving Leigh encephalopathy with infantile spasms in one sibling and Ohtahara syndrome in another are the only such cases reported so far (Tatsuno et al., 1984). Because we reported previously the polyalanine expansion mutation of *ARX* in two boys with Ohtahara syndrome (Kato et al., 2007), we considered *ARX* a strong candidate for being the causal factor in patients showing X-linked inheritance in this study. They had two novel frameshift mutations and an in-frame contraction mutation of *ARX*. The 9-bp deletion that shortens the first polyalanine tract by three residues was not found in the controls, although contractions of the polyalanine tract are generally considered not to be harmful (Brown & Brown, 2004; McKenzie et al., 2007), and it seems to be a rare polymorphism. Two other frameshift mutations exist in exon 5, which is the last exon of *ARX*. Premature termination mutations including a frameshift mutation from exon 1 to exon 4 of *ARX* cause malformation groups, such as lissencephaly, hydranencephaly, or agenesis of the corpus callosum (Kato et al., 2004). The length of the predicted mRNA is not correlated with the severity of the malformations, suggesting that nonsense-mediated mRNA decay (NMD) occurs (Kato & Dobyns, 2005). Interestingly, a sibship of two brothers with a total deletion of exon 5 showed infantile spasms but no brain malformation as in our patients (Stromme et al., 2002). The mutations existing in the last

exon of *ARX* are considered to cause NMD avoidance, indicating that it is a critical mechanism in the discrimination of brain malformation groups from nonmalformation groups in *ARX*-related diseases.

The mutations in our patients involved the Aristaless (or C-peptide domain), which consists of amino acids 526–542 in the human ARX (Kitamura et al., 2002). The *Xenopus* Arx protein functions as both a transcriptional activator and repressor in forebrain development (Seufert et al., 2005), and the human ARX protein is a potent transcriptional repressor (McKenzie et al., 2007). Although the fourth polyalanine tract and homeodomain serve as a repressor domain, the Aristaless domain works as an activator domain (McKenzie et al., 2007). The frameshift mutations in this study impair the Aristaless domain and enhance the original transcription repression activity of ARX; that is, they are gain-of-function mutations. On the contrary, the patient with a missense mutation (1561G>A, A521T) just before the Aristaless domain showed atypical XLAG, such as grade 1 lissencephaly and cerebellar hypoplasia (Kato et al., 2004). Although a functional study of each mutated protein needs to be performed to reveal the pathologic mechanism, frameshift mutations in exon 5 are likely to be pathogenic and causative for X-linked Ohtahara syndrome.

The patients in this study showed mild undescended testes or delayed puberty, but these symptoms are much milder than the micropenis displayed by patients with Ohtahara syndrome caused by the 33-bp expansion of the first polyalanine tract (Kato et al., 2007). The onset of seizures in this study occurred at 3 weeks to 2 months of age, whereas patients with the 33-bp expansion in the first polyalanine tract demonstrated their first seizure within a day of birth and tonic spasms at 1–3 weeks of age. The brain MRI of patients in this study also showed milder changes compared to the MRI findings of patients with 33-bp expansion in the first polyalanine tract, such as frontal-dominant lateral ventricular dilation, a thin corpus callosum, and delayed myelination (Kato et al., 2007). In addition, two patients carrying a large deletion of exon 5 demonstrated infantile spasms with hypsarrhythmia and severe developmental delay (Stromme et al., 2002). These findings suggest that frameshift mutations in exon 5, and possibly the deletion of exon 5, affect ARX function more mildly than the 33-bp expansion in the first polyalanine tract. A wide variety of *ARX*-related diseases, designated as interneuronopathies (Kato & Dobyns, 2005), are presumed to result from insufficiently controlled ARX function.

One of the patients in this study showed Lennox-Gastaut syndrome following Ohtahara syndrome and West syndrome. In many patients (~60%), Lennox-Gastaut syndrome is associated with underlying diseases, such as Down syndrome, brain malformations (Parrini et al., 2008), and sequelae of hypoxic encephalopathy or encephalitis; however, the etiology in other patients is still unknown. Recently, a mutation of the sodium channel alpha I subunit (*SCN1A*) gene, which is mainly responsible for severe myoclonic epilepsy of infancy or Dravet syndrome, has been found in one of 12 patients with Lennox-Gastaut syndrome (Harkin et al., 2007). Interestingly, male-predominant occurrence has been reported in patients with Lennox-Gastaut syndrome (Goldsmith et al., 2000; Trevathan et al., 1997). *ARX* causes Ohtahara syndrome and West syndrome in male patients and could be responsible for male Lennox-Gastaut syndrome patients with no known etiology.

In conclusion, the etiology of Ohtahara syndrome is heterogeneous; however, the molecular analysis of *ARX* should be considered in sporadic or familial male patients with Ohtahara syndrome.

Acknowledgments

This study was supported in part by research grants (18A-5 and 21B-6) for Nervous and Mental Disorders from the Ministry of Health, Labor and Welfare of Japan and a grant (19591198) for Grant-in-Aid for Scientific Research (C) from the Japan Society for the Promotion of Science (JSPS) to M Kato. We thank Keiko Tanaka, Yamagata University, for providing technical assistance.

Disclosure of Conflicts of Interest

Dr. Koyama, Dr. Ohta, Dr. Miura, and Dr. Hayasaka report no disclosures. We confirm that we have read the Journal's position on issues involved in ethical publication and affirm that this report is consistent with those guidelines.

References

Brown LY, Brown SA. (2004) Alanine tracts: the expanding story of human illness and trinucleotide repeats. *Trends Genet* 20:51–58.

Commission on Classification and Terminology of the International League Against Epilepsy. (1989) Proposal for revised classification of epilepsies and epileptic syndromes. *Epilepsia* 30:389–399.

Gecz J, Cloosterman D, Partington M. (2006) *ARX*: a gene for all seasons. *Curr Opin Genet Dev* 16:308–316.

Goldsmith IL, Zupanc ML, Buchhalter JR. (2000) Long-term seizure outcome in 74 patients with Lennox-Gastaut syndrome: effects of incorporating MRI head imaging in defining the cryptogenic subgroup. *Epilepsia* 41:395–399.

Guerrini R, Moro F, Kato M, Barkovich AJ, Shiihara T, McShane MA, Hurst J, Loi M, Tohyama J, Norci V, Hayasaka K, Kang UJ, Das S, Dobyns WB. (2007) Expansion of the first PolyA tract of ARX causes infantile spasms and status dystonicus. *Neurology* 69:427–433.

Harkin LA, McMahon JM, Iona X, Dibbens L, Pelekanos JT, Zuberi SM, Sadleir LG, Andermann E, Gill D, Farrell K, Connolly M, Stanley T, Harbord M, Andermann F, Wang J, Batish SD, Jones JG, Seltzer WK, Gardner A, Sutherland G, Berkovic SF, Mulley JC, Scheffer IE. (2007) The spectrum of *SCN1A*-related infantile epileptic encephalopathies. *Brain* 130:843–852.

Kato M, Das S, Petras K, Kitamura K, Morohashi K, Abuelo DN, Barr M, Bonneau D, Brady AF, Carpenter NJ, Cipero KL, Frisone F, Fukuda T, Guerrini R, Iida E, Itoh M, Lewanda AF, Nanba Y, Oka A, Proud VK, Saugier-Veber P, Schelley SL, Selicorni A, Shaner R, Silengo M, Stewart F, Sugiyama N, Toyama J, Toutain A, Vargas AL, Yanazawa M, Zackai EH, Dobyns WB. (2004) Mutations of *ARX* are associated with striking pleiotropy and consistent genotype-phenotype correlation. *Hum Mutat* 23:147–159.

Kato M, Dobyns WB. (2005) X-linked lissencephaly with abnormal genitalia as a tangential migration disorder causing intractable epilepsy:

proposal for a new term, "interneuronopathy". *J Child Neurol* 20:392–397.

Kato M. (2006) A new paradigm for West syndrome based on molecular and cell biology. *Epilepsy Res* 70(suppl 1):S87–S95.

Kato M, Saitoh S, Kamei A, Shiraishi H, Ueda Y, Akasaka M, Tohyama J, Akasaka N, Hayasaka K. (2007) A longer polyalanine expansion mutation in the *ARX* gene causes early infantile epileptic encephalopathy with suppression-burst pattern (Ohtahara syndrome). *Am J Hum Genet* 81:361–366.

Kitamura K, Yanazawa M, Sugiyama N, Miura H, Iizuka-Kogo A, Kusaka M, Omichi K, Suzuki R, Kato-Fukui Y, Kamiirisa K, Matsuo M, Kamijo S, Kasahara M, Yoshioka H, Ogata T, Fukuda T, Kondo I, Kato M, Dobyns WB, Yokoyama M, Morohashi K. (2002) Mutation of *ARX* causes abnormal development of forebrain and testes in mice and X-linked lissencephaly with abnormal genitalia in humans. *Nat Genet* 32:359–369.

McKenzie O, Ponte I, Mangelsdorf M, Finnis M, Colasante G, Shoubridge C, Stifani S, Gecz J, Broccoli V. (2007) *Aristaless*-related homeobox gene, the gene responsible for West syndrome and related disorders, is a Groucho/transducin-like enhancer of split dependent transcriptional repressor. *Neuroscience* 146:236–247.

Parrini E, Ferrari AR, Dorn T, Walsh CA, Guerrini R. (2008) Bilateral frontoparietal polymicrogyria, Lennox-Gastaut syndrome, and *GPR56* gene mutations. *Epilepsia* 50:1344–1353.

Saitsu H, Kato M, Mizuguchi T, Hamada K, Osaka H, Tohyama J, Uruno K, Kumada S, Nishiyama K, Nishimura A, Okada I, Yoshimura Y, Hirai S, Kumada T, Hayasaka K, Fukuda A, Ogata K, Matsumoto N. (2008) De novo mutations in the gene encoding STXBP1 (MUNC18-1) cause early infantile epileptic encephalopathy. *Nat Genet* 40:782–788.

Seufert DW, Prescott NL, El-Hodiri HM. (2005) *Xenopus aristaless-related homeobox* (*xARX*) gene product functions as both a transcriptional activator and repressor in forebrain development. *Dev Dyn* 232:313–324.

Starke H, Seidel J, Henn W, Reichardt S, Volleth M, Stumm M, Behrend C, Sandig KR, Kelbova C, Senger G, Albrecht B, Hansmann I, Heller A, Claussen U, Liehr T. (2002) Homologous sequences at human chromosome 9 bands p12 and q13-21.1 are involved in different patterns of pericentric rearrangements. *Eur J Hum Genet* 10:790–800.

Stromme P, Mangelsdorf ME, Shaw MA, Lower KM, Lewis SM, Bruyere H, Lutcherath V, Gedeon AK, Wallace RH, Scheffer IE, Turner G, Partington M, Frints SG, Fryns JP, Sutherland GR, Mulley JC, Gecz J. (2002) Mutations in the human ortholog of *Aristaless* cause X-linked mental retardation and epilepsy. *Nat Genet* 30:441–445.

Tatsuno M, Hayashi M, Iwamoto H, Sasaki Y, Hara M. (1984) [Autopsy case of Leigh's encephalopathy with wide lesions in central nervous system and early infantile epileptic encephalopathy with burst suppression]. *No To Hattatsu* 16:68–75.

Trevathan E, Murphy CC, Yeargin-Allsopp M. (1997) Prevalence and descriptive epidemiology of Lennox-Gastaut syndrome among Atlanta children. *Epilepsia* 38:1283–1288.

Yamatogi Y, Ohtahara S. (2002) Early-infantile epileptic encephalopathy with suppression-bursts, Ohtahara syndrome; its overview referring to our 16 cases. *Brain Dev* 24:13–23.

Supporting Information

Additional Supporting Information may be found in the online version of this article:

Figure S1. Electroencephalography (EEG) of Patient 2. At the age of 43 days, an interictal EEG showed a suppression-burst pattern in both the awake (**A**) and asleep states (**B**), which was typical for Ohtahara syndrome. An ictal EEG of myoclonic seizures (**C**, arrows) showed diffuse irregular polyspike-and-slow waves. An EEG after 15 days of adrenocorticotropic hormone (ACTH) injection at 3 months showed multifocal spikes both in the awake and asleep states (**D**).

Please note: Wiley-Blackwell is not responsible for the content or functionality of any supporting information supplied by the authors. Any queries (other than missing material) should be directed to the corresponding author for the article.

ELSEVIER

Brain & Development 32 (2010) 695–702

BRAIN & DEVELOPMENT
Official Journal of the Japanese Society of Child Neurology

www.elsevier.com/locate/braindev

Original article

Peripheral lymphocyte subset and serum cytokine profiles of patients with West syndrome

Takashi Shiihara [a,b,*], Momoyo Miyashita [c], Masakazu Yoshizumi [d], Mio Watanabe [a], Yoshiyuki Yamada [e], Masahiko Kato [e]

[a] *Department of Neurology, Gunma Children's Medical Center, 779 Shimohakoda Hokkitsu-machi, Shibukawa, Gunma 377-8577, Japan*
[b] *Department of Pediatrics, Dokkyo Medical University, Koshigaya Hospital, 2-1-50 Minami-Koshigaya, Koshigaya, Saitama 343-8555, Japan*
[c] *Department of Laboratory Medicine, Gunma Children's Medical Center, 779 Shimohakoda, Hokkitsu-machi, Shibukawa, Gunma 377-8577, Japan*
[d] *Gunma Prefectural Institute of Public Health and Environmental Sciences, 378 Kamioki, Maebashi, Gunma 371-0052, Japan*
[e] *Department of Allergy and Immunology, Gunma Children's Medical Center, 779 Shimohakoda, Hokkitsu-machi, Shibukawa, Gunma 377-8577, Japan*

Received 27 August 2009; received in revised form 21 October 2009; accepted 2 November 2009

Abstract

Objective: To clarify the immune pathophysiology of West syndrome (WS). *Study design:* We measured peripheral blood lymphocyte subset and serum cytokine profiles in 76 WS patients and 26 age-matched controls. Adrenocorticotropic hormone (ACTH) is one of the most effective therapy for WS and presumably immune-modulating; therefore, we compared the measured parameters between before ACTH (pre-ACTH) WS patients and controls, between cryptogenic and symptomatic WS patients before ACTH (pre-ACTH), and between before (pre-ACTH) and after (post-ACTH) ACTH WS patients. The post-ACTH group included those who received the last ACTH dose within 1 month of sampling. *Results:* CD3+ CD25+, CD19+, and CD19+ CD95+ cells were found to be significantly lower in the pre-ACTH group than in the controls. Interleukin (IL)-1 receptor antagonist (RA), 5, 6, and 15; eotaxin; basic fibroblast growth factor (bFGF); and interferon γ-inducible protein (IP)-10 levels were higher in pre-ACTH group than in the controls. No significant differences were found between the pre-ACTH cryptogenic and symptomatic groups. CD4+ cells, CD3+ cells, CD4+/8+ ratio, IL-1β, IL-12, and macrophage inflammatory protein (MIP)-1β were significantly higher in pre-ACTH group than in the post-ACTH group. *Conclusions:* Our study revealed immunological alterations in WS patients, and these responses were modified by ACTH therapy. Further study is needed to elucidate whether or how the immune system alteration is involved in the pathophysiology of WS.

Keywords: Lymphocyte subset; Cytokine; West syndrome; Adrenocorticotropic hormone; Fas; Regulatory T-cells

1. Introduction

West syndrome (WS) is recognized as an epileptic syndrome in infancy and is characterized by brief tonic spasms, peculiar electroencephalographic findings termed as hypsarrhythmia, and arrest or regression of psychomotor development [1]. Many etiological factors of WS, including hereditary and non-hereditary conditions, such as neonatal asphyxia, meningoencephalitis, cerebral dysgenesis, and congenital metabolic disorders, have been reported. This syndrome is now classified into 2 groups: symptomatic and cryptogenic (International League Against Epilepsy Task Force, 1989. Available from: http://www.ilae-epilepsy.org/ctf/). Symptomatic WS is characterized by the presence of previous signs of brain damage (psychomotor retardation, neurological

* Corresponding author. Address: Department of Neurology, Gunma Children's Medical Center, 779 Shimohakoda Hokkitsu-machi, Shibukawa, Gunma 377-8577, Japan. Tel.: +81 279 52 3551; fax: +81 279 52 2045.
E-mail address: shiihara-ind@umin.net (T. Shiihara).

0387-7604/$ - see front matter © 2009 Elsevier B.V. All rights reserved.
doi:10.1016/j.braindev.2009.11.001

signs, radiological signs, or other types of seizures) or by a known etiology. However, the cryptogenic group is not characterized by these features.

Another characteristic feature of WS is the relative high therapeutic efficacy of immune suppressants such as adrenocorticotropic hormone (ACTH) or glucocorticoids [2,3]. Moreover, spontaneous remission following acute viral infections has also been reported [4]. On the basis of these findings, it is plausible that some immune mechanisms play certain pathophysiological roles in WS. To date, there have been several reports on the immunological aspects of WS [5–9]; however, the exact mechanisms remain unknown. The initial response to ACTH therapy is usually favorable, and cessation of tonic spasm has been observed in more than 90% of the patients; however, relapse and side effects are not uncommon and occur in more than 40% and 80% of the patients, respectively [10]. Therefore, in order to clarify the immune pathophysiology of WS, we investigated the peripheral blood lymphocyte subset and serum cytokine profiles of patients with WS.

2. Methods

2.1. Patients and controls

From November 2006 to August 2008, WS patients were enrolled mainly via mailing lists for Japanese pediatric neurologists or pediatricians, such as the Zao Seminar Mailing List (available from: http://square.umin.ac.jp/shiihara/) and Japan Pediatric Mailing List Conferences (available from: http://jpmlc.org/). The diagnosis of WS was confirmed either by observation of brief tonic spasms and hypsarrhythmia by an attending physician or on the basis of other available clinical information. The patients were under no obligation to undergo WS therapy. The control group consisted of patients from the Gunma Children's Medical Center (GCMC) who were less than 2 years old, without acute illness or any other immune-mediated disorders. Approval from the GCMC institutional review board and written informed consents were obtained from the parents of patients and controls.

Seventy six patients with WS (37 boys and 39 girls; mean age, 7.9 months old; age range, 3–26 months old) were enrolled in this study. These included 32 patients with cryptogenic WS and 44 with symptomatic WS. Among 44 symptomatic WS patients, there were no overt congenital infections, except 1 girl with congenital cytomegalovirus infection, who was 11 month-old at enrollment without any sign of active cytomegalovirus infection. The control group consisted of 26 patients (8 boys and 18 girls; mean age, 10.5 months old; age range, 2–23 months old) without WS and other overt immune-mediated disorders and infections. Blood was sampled from the WS patients both before (pre-ACTH) and after ACTH (post-ACTH) therapy. The post-ACTH group included patients who received the last ACTH dose within 1 month of sampling. There was no definite period during which blood sampling was carried out in the control group. Indeed, some of the WS patients did not receive ACTH therapy, and blood samples for the analyses of both lymphocyte subsets and serum cytokines in the pre- and post-ACTH groups could not be obtained for all WS patients.

2.2. Lymphocyte subsets

Peripheral venous blood was withdrawn from each patient, placed into a tube containing ethylenediaminetetraacetic acid (EDTA), and delivered to our laboratory as soon as possible. Lymphocyte subsets examination was performed usually within 30 h of blood draw. Absolute lymphocyte counts were determined as the product of the white blood cell count and percent lymphocyte differential measured by using hematology instruments. For specimen preparation, 100 μl of EDTA-anticoagulated blood was incubated with premixed antibodies for 15 min, and the erythrocytes were lysed using OptiLyse C (Beckman Coulter Inc., Fullerton, CA, USA). Lymphocyte subsets were analyzed by using an EPICS-XL-MCL coulter with data acquisition software (Beckman Coulter). The following mouse anti-human monoclonal antibodies were used: cluster designation (CD) 3-fluorescein isothiocyanate (FITC)/CD19-phycoerythrin (PE), CD3-FITC/CD56-PE, CD4-FITC/CD8-PE, CD3-proprotein convertase (PC)5, CD19-PC5, CD23-FITC, CD25-FITC, CD40-PE, CD69-PE, and CD95-PE (Beckman Coulter). We measured the counts of CD8+ (cytotoxic T), CD4+ (helper T), CD19+ (B), CD3+ (T), CD3− CD56+ (natural killer), CD3+ CD69+ (activated T), CD3+ CD25+ (activated T), CD3+ CD95+ (Fas-positive T), CD19+ CD23− CD40+ (activated B), CD19+ CD23+ CD40+ (activated B), and CD19+ CD95+ (Fas-positive B) cells [10]. In addition, we also calculated the CD4+/8+ ratio. The analysis was preformed according to the manufacturer's instructions (available from: http://www.coulterflow.com/).

2.3. Cytokine assay

Serum cytokines were stored at −80 °C until use and analyzed using a multiplex bead-based immunoassay system (Bio-Plex Human Cytokine 27-Plex Panel; Bio-Rad Laboratories Inc., Hercules, CA, USA) that contained the following cytokines, chemokines, and growth factors: interleukin (IL)-1β, IL-1 receptor antagonist (RA), IL-2, 4, 5, 6, 7, 8, 9, 10, 12 (p70), 13, 15, and 17; eotaxin; basic fibroblast growth factor (bFGF); granulocyte colony-stimulating factor; granulocyte macrophage colony-stimulating factor; interferon (IFN)-γ;

IFN-γ-inducible protein (IP)-10; monocyte chemotactic protein-1; macrophage inflammatory protein (MIP)-1α and 1β; platelet-derived growth factor-BB; regulated upon activation T-cell expressed and secreted; tumor necrosis factor (TNF)-α; and vascular endothelial growth factor. We calculated the IFN-γ/IL-4, IFN-γ/IL-5, IFN-γ/IL-10, and IFN-γ/IL-13 ratios that represent the T helper 1 (Th1)/T helper 2 (Th2) cytokine balance. The analysis was performed according to the manufacturer's instructions (available from: http://www.bio-rad.com/). Patient serum was diluted in buffer to obtain a 1:4 dilution, and 50 μl was added to the washed, fluorescently dyed microspheres (beads) to which the biomolecules of interest were bound. The beads and the diluted patient serum were incubated for 30 min at room temperature with agitation. After incubation, the beads were washed in Bio-Plex wash buffer and incubated with 25 μl of the detection antibody for 30 min as described above. After washing, the beads were incubated with streptavidin–PE and washed a final time. The bound beads were resuspended in 125 μl of the Bio-Plex assay buffer and were analyzed using the Bio-Plex suspension array system (Bio-Rad).

2.4. Statistical analysis

Data were expressed as the mean ± standard deviation (SD), unless otherwise specified. Statistical analyses were performed using the statistical package R version 2.9.0 (available as a free download from http://www.r-project.org). Numerical variables were compared using the Wilcoxon rank sum test. A P value less than 0.05 was considered statistically significant.

3. Results

Initially, the white blood cell, lymphocyte, lymphocyte subset, and serum cytokine counts were compared between the pre-ACTH groups and the controls. Significant differences were found with regard to CD3+ CD25+, CD19+, and CD19+ CD95+ cells; IL-1RA, 5, 6, and 15; eotaxin; bFGF; and IP-10 levels. The lymphocyte subset counts were lower in the pre-ACTH group ($n = 33$) than in the controls ($n = 24$) (CD3+ CD25+ cells: 326 ± 136 vs. 400 ± 129 cells/μl, $p = 0.02947$; CD19+ cells: 1407 ± 732 vs. 1778 ± 522 cells/μl, $p = 0.01142$; CD19+ CD95+ cells: 303 ± 249 vs. 676 ± 422 cells/μl, $p < 0.0001$, respectively), while cytokines were higher in the pre-ACTH group ($n = 75$) than in the controls ($n = 26$) (IL-1RA: 747.6 ± 1491.4 vs. 545.7 ± 1247.1 pg/ml, $p = 0.04719$; IL-5: 6.3 ± 26.4 vs. 2.0 ± 2.3 pg/ml, $p = 0.01121$; IL-6: 30.9 ± 49.3 vs. 19.1 ± 32.8 pg/ml, $p = 0.005359$; IL-15: 16.1 ± 24.8 vs. 9.9 ± 22.7 pg/ml, $p = 0.03024$; eotaxin: 88.1 ± 72.3 vs. 57.9 ± 46.6 pg/ml, $p = 0.002269$; bFGF: 26.5 ± 42.3 vs. 5.2 ± 13.6 pg/ml, $p = 0.007362$; IP-10: 1294.0 ± 1239.9 vs. 654.3 ± 539.6 pg/ml, $p = 0.0008737$, respectively) (Fig. 1).

Next, the white blood cell, lymphocyte, lymphocyte subset, and serum cytokine subset counts were compared between cryptogenic and symptomatic WS patients. There were no statistically significant differences with regard to either lymphocyte subsets (cryptogenic pre-ACTH group ($n = 12$) vs. symptomatic pre-ACTH group ($n = 21$)) and serum cytokines (cryptogenic pre-ACTH group ($n = 30$) vs. symptomatic pre-ACTH group ($n = 45$)) (data not shown).

Finally, we compared the white blood cell, lymphocyte, lymphocyte subset, and serum cytokine counts between the pre- and post-ACTH groups. Significant differences were found with regard to CD4+ and CD3+ cells, CD4+/8+ ratio, IL-1β, IL-12, and MIP-1β. These levels were higher in the pre-ACTH group than in the post-ACTH group: lymphocyte subsets (pre- and post-ACTH groups ($n = 16$)) (CD4+ cells: 2355 ± 1181 vs. 1493 ± 749 cells/μl, $p = 0.01864$; CD3+ cells: 3654 ± 1558 vs. 2639 ± 1062 cells/μl, $p = 0.03624$; CD4+/8+ ratio: 2.10 ± 1.00 vs. 1.42 ± 0.68, $p = 0.003483$, respectively) and cytokines (pre- and post-ACTH WS ($n = 27$)) (IL-1β: 6.5 ± 8.1 vs. 4.1 ± 1.3 pg/ml, $p = 0.002248$; IL-12: 26.5 ± 42.0 vs. 13.9 ± 11.9 pg/ml, $p = 0.03853$; MIP-1β: 300.6 ± 260.3 vs. 236.8 ± 160.8 pg/ml, $p = 0.0491$, respectively) (Fig. 2).

4. Discussion

In the present study, CD3+ CD25+ cells, CD19+ cells, and CD19+ CD95+ cells were decreased in the pre-ACTH group as compared to the controls, whereas IL-1RA, 5, 6, and 15; eotaxin; bFGF; and IP-10 were increased in the pre-ACTH group as compared to the controls.

Initially, we investigated the changes in the peripheral lymphocyte subset levels. CD3+ CD25+ cells comprehend regulatory T-cells (Tregs), a recently recognized member of the Th repertoire that is essential for maintaining peripheral tolerance, thus preventing autoimmune diseases and limiting chronic inflammatory diseases [11,12]. The levels of Tregs in the peripheral blood are reduced in the acute phase of some autoimmune disorders such as Guillain–Barré syndrome and myasthenia gravis, and these levels improved with immune-modulating therapy [13,14]. Moreover, CD95+, also called Fas, belongs to the subgroup of the TNF receptor family; it contains an intracellular death domain and triggers apoptosis [11,15]. Thus, reduced levels of CD19+ CD95+ cells could indicate reduced B-cell apoptosis in the pre-ACTH group. B-cell apoptosis plays a role in the elimination of self-reactive B-cells, which is an essential process for self-tolerance [11,16,17]. Further, B-cells have been recognized to play

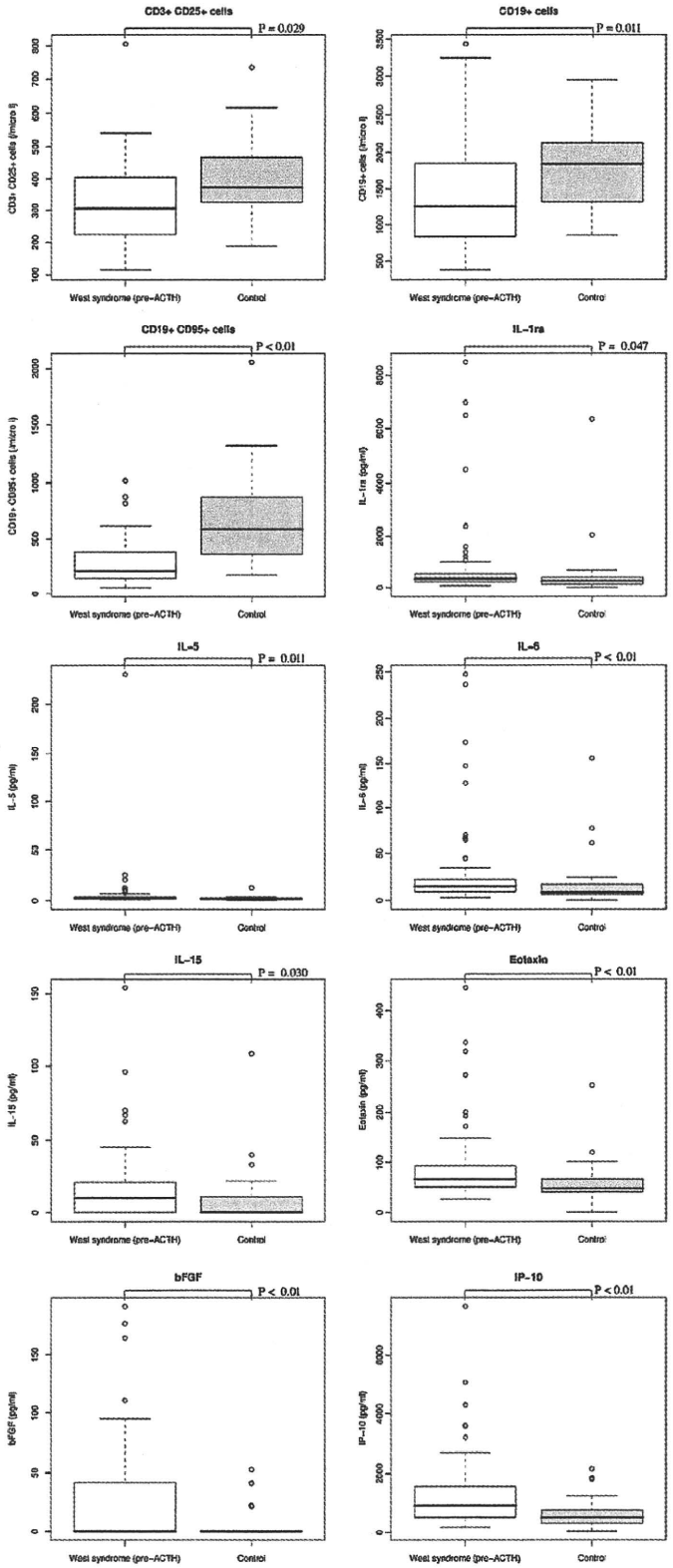

Fig. 1. Lymphocyte subsets and cytokines in the pre-ACTH group and controls. Box and whisker plot of lymphocyte subsets and serum cytokines in the pre-ACTH group and controls. Center lines denote medians, boxes denote 25–75% percentiles, and whiskers denote the minimum and maximum values (white circles denote outliers, if any present). Statistical comparisons between the pre-ACTH group and controls were analyzed by the Wilcoxon rank sum test. Only the parameters with statistically significant differences are shown.

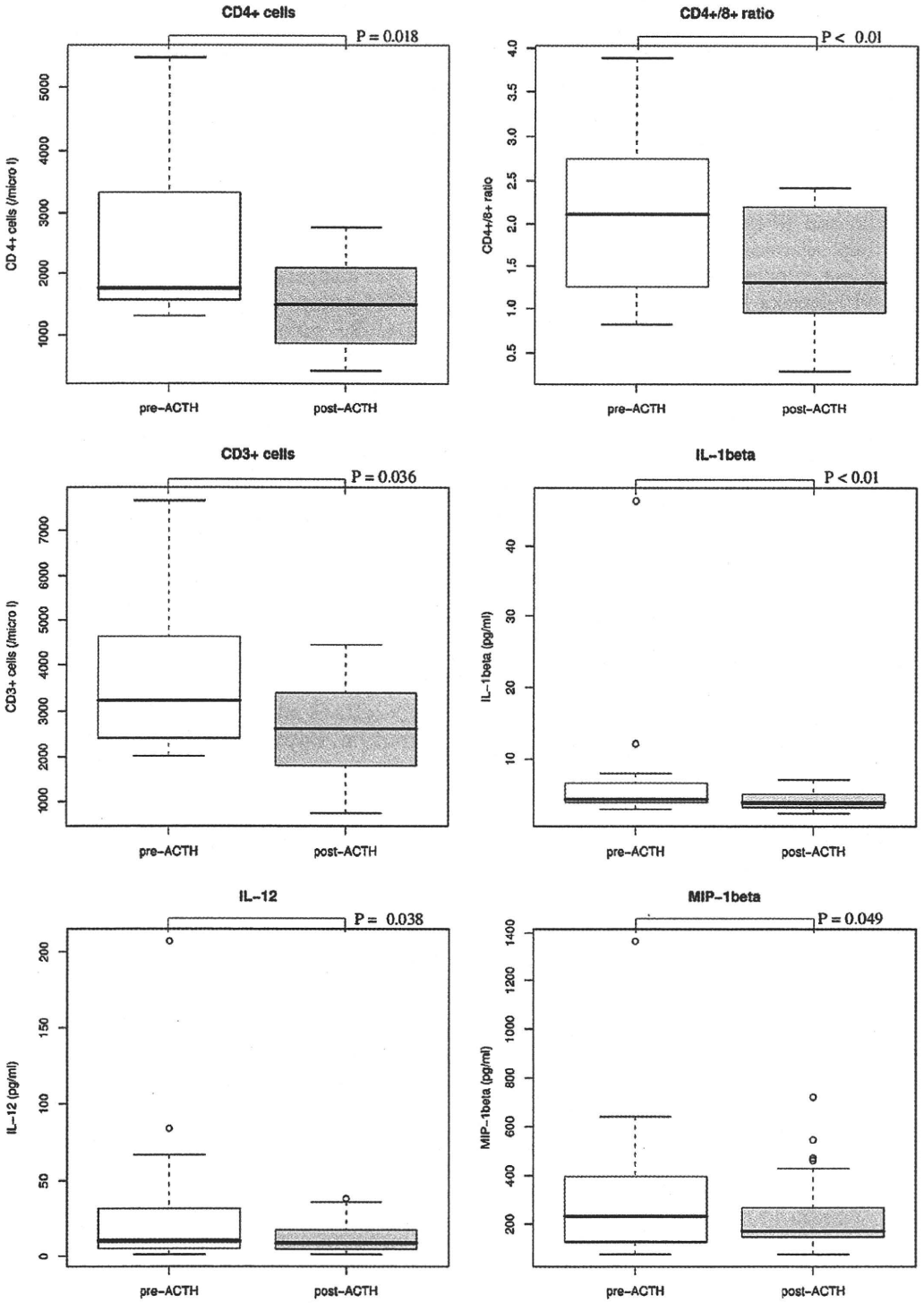

Fig. 2. Lymphocyte subsets and cytokines in the pre- and post-ACTH groups. Box and whisker plot of lymphocyte subsets and serum cytokines in the pre- and post-ACTH groups. Center lines denote medians, boxes denote 25–75% percentiles, and whiskers denote the minimum and maximum values (white circles denote outliers, if any present). Statistical comparisons between the pre- and post-ACTH WS patients were analyzed by the Wilcoxon rank sum test. Only the parameters with statistically significant differences are shown.

a pivotal role in some autoimmune disorders such as rheumatoid arthritis and multiple sclerosis [18,19]. In experimental autoimmune encephalomyelitis, B-cells were eliminated from the central nervous system (CNS) by CD95- or Fas-mediated B-cell apoptosis, which contributed to the spontaneous resolution of

CNS inflammation and clinical recovery [20,21]. Thus, reduced levels of CD3+ CD25+ cells and CD19+ CD95+ cells observed in the pre-ACTH group might be associated with the pathogenesis of WS.

Next, we would like to investigate the changes in the serum cytokine levels. Previous studies on some autoimmune disorders and organ transplantations showed similar increases in the levels of cytokines such as IL-1RA, 5, and 6; eotaxin; and IP-10 in the cerebrospinal fluid (CSF) in multiple sclerosis or neuromyelitis optica, increases in IL-5 and eotaxin in corneal xenograft rejection in mice, and increases in IP-10 in type 1 diabetes and allograft rejection [22–26]. IL-5 and 6 are produced by T-cells, and thus their elevations could indicate T-cell activation [11]. Target cells for eotaxin include eosinophils and Th2 cells [11]. On the other hand, the target cells for IP-10 include activated T-cells (a greater proportion of Th1 than Th2) and B-cells [11]. These results could reflect the activations of not only T-cells but also B-cells in WS. In addition, bFGF is a potent angiogenic factor and endothelial cell mitogen that potentiates leukocyte recruitment and may play a role in lymphocyte recruitment into the brain of WS patients [27].

The differences in the measured lymphocyte subsets and serum cytokines between the pre-ACTH cryptogenic and symptomatic groups were not statistically significant. WS is usually categorized as cryptogenic or symptomatic depending on whether the patient exhibits overt pathology or not. Because of the advancements in brain imaging and genetic research, there seems to be an increase in the number of symptomatic WS patients that were formerly categorized as cryptogenic. Indeed, previously unknown responsible genes such as *ARX* and *CDKL5* have been identified in cryptogenic WS [1]. The line of differentiation between cryptogenic and symptomatic WS was not very obvious, and there was no clear differentiation between cryptogenic and symptomatic WS, at least, with regard to the immunological parameters examined.

The comparison between the pre-ACTH and post-ACTH groups revealed that CD4+ cells, CD3+ cells, CD4+/8+ ratio, IL-1β, IL-12, and MIP-1β decreased during ACTH therapy. The CD4+ cell reduction was in agreement with previous studies in WS on through ACTH therapy and Cushing's syndrome with an increase in hypothalamic–pituitary-adrenal axis hormones [9,28]. To the best of our knowledge, this is the first study on plasma cytokine response to ACTH in WS patients. IL-1β, IL-12, and MIP-1β could activate T-cells [11]. These results suggest that ACTH could cause T-cell inactivation, however, the precise role in its therapeutic effect is still uncertain.

The comparisons between the 2 groups did not reveal a statistically significant Th1/Th2 cytokine imbalance, in terms of the IFN-γ/IL-4, IFN-γ/IL-5, IFN-γ/IL-10, and IFN-γ/IL-13 ratios. According to the classical Th1/Th2 paradigm, excessive Th1 responses are associated with various autoimmune and inflammatory disorders,

Table 1
Summary of WS immunological studies.

References	Number of WS patients	Number of controls	Principal parameters	Main findings in WS	
				Elevated	Reduced
Liu et al. [5]	23	15	Serum cytokines; IL-2, TNF-α, and IFN-α	IL-2,TNF-α and lFN-α	
Montelli et al. [7]	50 (including 17 post-WS[a])	20	Peripheral lymphocyte subsets; CD1+ cells, CD3+ cells, CD4+ cells, CD8+ cells, and CD4+/CD8+ ratio	CD8+ cells	CD3+ cells. CD4+ cells and CD4+/8+ ratio
Tekgul et al. [6]	12	12 (bacterial meningitis/encephalitis) and 5 (post-traumatic seizures)	CSF IL-6		IL-6
Haginoya el al [8]	24	13	CSF IL-lβ, IL-1RA, IL-6, and TNF-α		IL-1RA
Ohya et al. [9]	18	0	Peripheral lymphocyte subsets; CD4+ cells, CD8+ cells, and CD 4+/8+ ratio		CD4+ cells (along ACTH therapy)
Present study	76	26	Peripheral lymphocyte subsets and serum cytokines (refer to the text)	IL-1RA, IL-5, IL-6, IL-15, eotaxin, bFGF, and IP-10	CD3+ CD25+ cells and CD19_ CD95+ cells

Abbreviations: IL = interleukin; TNF = tumor necrosis factor; IFN = interferon; ACTH = adrenocorticotropic hormone; CD = cluster designation; WS = West syndrome, RA = receptor antagonist; bFGF = basic fibroblast growth factor; IP = IFN-γ-inducible protein.

[a] Post-WS designate patients initially diagnosed WS later evolving to other epilepsy such as Lennox–Gastaut syndrome.

whereas enhanced Th2 cytokine production is involved in atopic diseases, including allergies and asthma [11,29,30]. The results of our study did not implicate the Th1/Th2 paradigm in WS.

During this decade, several researches have been conducted on the immunologic aspects of WS, and the results have been inconclusive (Table 1) [5–9]. Each study had its own limitations. Liu et al. reported significant increases in serum IL-2, TNF-α, and IFN-α in WS; however, other parameters were not examined [5]. The study by Montelli et al. included 17 post-WS patients who were initially diagnosed with WS that later evolved into other epileptic conditions such as Lennox–Gastaut syndrome, which could have affected the results of the study [7]. Tekgul et al. could not obtain CSF from the presumably healthy control group and only included CSF samples from the inflammatory or traumatic groups [6]. Haginoya et al. measured IL-1β, IL-1RA, IL-6, and TNF-α in CSF and there were no significant changes of these cytokines except reduced levels of IL-1RA in WS [8]. Ohya et al. did not include a control group [9]. In present study, we also had some flaws. We considered that reduced CD3+ CD25+ cell levels possibly indicate reduced Tregs; however, CD4+, CD25+, and forkhead box protein 3 are needed for the precise identification of Tregs [11,12]. Furthermore, we interpreted the reduced CD19+ CD95+ levels as reduced B-cell apoptosis; however, there was no direct testing for B-cell apoptosis. In summary, our study might suggest that T-cell and B-cell activation have some role in WS, and ACTH therapy may associate with T-cell inactivation. Unfortunately, the results of present study does not fully coincide with that of the previously published studies. They could be partly due to the fact that each study used different patients group, different controls if available, different specimens, and different parameters. Beyond the methodological concerns, it is also possible that the immune status alteration is a mere consequence, not the cause, of WS. Further study is needed to elucidate whether or how the immune system alteration is involved in the pathophysiology of WS.

Acknowledgments

This study was supported by the Medical Research Program of Gunma Prefectural Government, Japan. We are deeply grateful to all the patients, their parents, and doctors who participated in this study.

References

[1] Kato M. A new paradigm for West syndrome based on molecular and cell biology. Epilepsy Res 2006;70(Suppl. 1):S87–95.
[2] Yamamoto H, Fukuda M, Miyamoto Y, Murakami H, Kamiyama N. A new trial liposteroid (dexamethasone palmitate) therapy for intractable epileptic seizures in infancy. Brain Dev 2007;29:421–4.
[3] Tsuji T, Okumura A, Ozawa H, Ito M, Watanabe K. Current treatment of West syndrome in Japan. J Child Neurol 2007;22:560–4.
[4] Sugiura C, Maegaki Y, Kure H, Inoue T, Ohno K. Spontaneous remission of infantile spasms and hypsarrhythmia following acute infection with high-grade fever. Epilepsy Res 2007;77:102–7.
[5] Liu Z, Wang Q, Wang F, Yang L. Serum cytokine levels are altered in patients with West syndrome. Brain Dev 2001;23:548–51.
[6] Tekgul H, Polat M, Tosun A, Serdaroglu G, Kutukculer N, Gokben S. Cerebrospinal fluid interleukin-6 levels in patients with West syndrome. Brain Dev 2006;28:3–19.
[7] Montelli TCB, Soares AMVC, Pera C'oli MTS. Immunologic aspects of West syndrome and evidence of plasma inhibitory effects on T cell function. Arq Neuropsiquiatr 2003;61:731–7.
[8] Haginoya K, Noguchi R, Zhao Y, Munakata M, Yokoyama H, Tanaka S, et al. Reduced levels of interleukin-1 receptor antagonist in the cerebrospinal fluid in patients with West syndrome. Epilepsy Res 2009;85:314–7.
[9] Ohya T, Nagai T, Araki Y, Yanagawa T, Tanabe T, Iyoda K, et al. A pilot study on the changes in immunity after ACTH therapy in patients with West syndrome. Brain Dev, in press, doi:10.1016/j.braindev.2008.11.007.
[10] Kondo Y, Okumura A, Watanabe K, Negoro T, Kato T, Kubota T, et al. Comparison of two low dose ACTH therapies for West syndrome: their efficacy and side effect. Brain Dev 2005;27:326–30.
[11] Murphy KM, Travers P, Walport M. Janeway's Immunobiology. 7th ed. New York and London: Garland Science; 2007.
[12] Vignali DAA, Collison LW, Workman CJ. How regulatory T cells work. Nat Rev Immunol 2008;8:523–32.
[13] Fattorossi A, Battaglia A, Buzzonetti A, Ciaraffa F, Scambia G, Evoli A. Circulating and thymic CD4 CD25 T regulatory cells in myasthenia gravis: effect of immunosuppressive treatment. Immunology 2005;116:134–41.
[14] Chi L, Wang H, Zhang Y, Wang W. Abnormality of circulating CD4(+)CD25(+) regulatory T cell in patients with Guillain–Barré syndrome. J Neuroimmunol 2007;192:206–14.
[15] Strasser A, Jost PJ, Nagata S. The many roles of FAS receptor signaling in the immune system. Immunity 2009;30:180–92.
[16] Yan B, Adachi T, Tsubata T. ER stress is involved in B cell antigen receptor ligation-induced apoptosis. Biochem Biophys Res Commun 2008;365:143–8.
[17] Strasser A, Puthalakath H, O'Reilly LA, Bouillet P. What do we know about the mechanisms of elimination of autoreactive T and B cells and what challenges remain. Immunol Cell Biol 2008;86:57–66.
[18] Bugatti S, Codullo V, Caporali R, Montecucco C. B cells in rheumatoid arthritis. Autoimmun Rev 2007;6:482–7.
[19] Oh S, Cudrici C, Ito T, Rus H. B-cells and humoral immunity in multiple sclerosis. Implications for therapy. Immunol Res 2008;40:224–34.
[20] Suvannavejh GC, Canto MCD, Matis LA, Miller SD. Fas-mediated apoptosis in clinical remissions of relapsing experimental autoimmune encephalomyelitis. J Clin Invest 2000;105:223–31.
[21] White CA, Nguyen KB, Pender MP. B cell apoptosis in the central nervous system in experimental autoimmune encephalomyelitis: roles of B cell CD95, CD95L and Bcl-2 expression. J Autoimmun 2000;14:195–204.
[22] Correale J, Fiol M. Activation of humoral immunity and eosinophils in neuromyelitis optica. Neurology 2004;63:2363–70.
[23] Tanaka M, Matsushita T, Tateishi T, Ochi H, Kawano Y, Mei F, et al. Distinct CSF cytokine/chemokine profiles in atopic myelitis and other causes of myelitis. Neurology 2008;71:974–81.

[24] Tanaka K, Yamagami S, Streilein JW. Evidence that T-helper type 2 cell-derived cytokines and eosinophils contribute to acute rejection of orthotopic corneal xenografts in mice. Transplantation 2005;79:1317–23.
[25] Nakagawa Y, Shimada A, Oikawa Y, Irie J, Shigihara T, Tsumura K, et al. Two cases of "fulminant" type 1 diabetes suggesting involvement of autoimmunity. Ann N Y Acad Sci 2003;1005: 359–61.
[26] Christen U, von Herrath MG. IP-10 and type 1 diabetes: a question of time and location. Autoimmunity 2004;37:273–82.
[27] Zittermann SI, Issekutz AC. Basic fibroblast growth factor (bFGF, FGF-2) potentiates leukocyte recruitment to inflammation by enhancing endothelial adhesion molecule expression. Am J Pathol 2006;168:835–46.
[28] Kronfol Z, Starkman M, Schteingart DE, Singh V, Zhang Q, Hill E. Immune regulation in Cushing's syndrome: relationship to hypothalamic–pituitary-adrenal axis hormones. Psychoneuroendocrinology 1996;21:599–608.
[29] van Oosterhout AJM, Motta AC. Th1/Th2 paradigm: not seeing the forest for the trees? Eur Respir J 2005;25:591–3.
[30] Gutcher I, Becher B. APC-derived cytokines and T cell polarization in autoimmune inflammation. J Clin Invest 2007;117:1119–27.

RESEARCH ARTICLE

Human Mutation

OFFICIAL JOURNAL
HGVS
HUMAN GENOME VARIATION SOCIETY
www.hgvs.org

Molecular and Clinical Analysis of *RAF1* in Noonan Syndrome and Related Disorders: Dephosphorylation of Serine 259 as the Essential Mechanism for Mutant Activation

Tomoko Kobayashi,[1] Yoko Aoki,[1]* Tetsuya Niihori,[1] Hélène Cavé,[2] Alain Verloes,[2] Nobuhiko Okamoto,[3] Hiroshi Kawame,[4,5] Ikuma Fujiwara,[6] Fumio Takada,[7] Takako Ohata,[7] Satoru Sakazume,[8] Tatsuya Ando,[9] Noriko Nakagawa,[10] Pablo Lapunzina,[11] Antonio G. Meneses,[11] Gabriele Gillessen-Kaesbach,[12] Dagmar Wieczorek,[13] Kenji Kurosawa,[14] Seiji Mizuno,[15] Hirofumi Ohashi,[16] Albert David,[17] Nicole Philip,[18] Afag Guliyeva,[1] Yoko Narumi,[1] Shigeo Kure,[1,6] Shigeru Tsuchiya,[6] and Yoichi Matsubara[1]

[1]Department of Medical Genetics, Tohoku University School of Medicine, Sendai, Japan; [2]APHP, Hôpital Robert Debré, Département de Génétique; Université Paris 7-Denis Diderot, Paris, France; [3]Department of Medical Genetics, Osaka Medical Center and Research Institute for Maternal and Child Health, Izumi, Osaka, Japan; [4]Division of Medical Genetics, Nagano Children's Hospital, Nagano, Japan; [5]Department of Genetic Counseling, Ochanomizu University, Tokyo, Japan; [6]Department of Pediatrics, Tohoku University School of Medicine, Sendai, Japan; [7]Department of Medical Genetics, Kitasato University Graduate School of Medical Sciences, Sagamihara, Japan; [8]Division of Medical Genetics, Gunma Children's Medical Center, Gunma, Japan; [9]Department of Pediatrics, Jikei University School of Medicine, Tokyo, Japan; [10]Department of Pediatrics, National Defense Medical College, Tokorozawa, Saitama, Japan; [11]Servicio de Genetica Medica, Hospital Universitario La Paz, Madrid, Spain; [12]Institut für Humangenetik Lübeck, Universitätsklinikum Schleswig-Holstein, Lübeck, Germany; [13]Institut für Humangenetik, Universitaetsklinikum Essen Universitaet Duisburg-Essen, Essen, Germany; [14]Division of Medical Genetics, Kanagawa Children's Medical Center, Yokohama, Japan; [15]Department of Pediatrics, Central Hospital, Aichi Human Service Center, Aichi, Japan; [16]Division of Medical Genetics, Saitama Children's Medical Center, Saitama, Japan; [17]CHU Nantes, Nantes, France; [18]Hôpital de la Timone, Marseille, France

Communicated by Nancy B. Spinner

Received 20 July 2009; accepted revised manuscript 2 December 2009.
Published online 5 January 2010 in Wiley InterScience (www.interscience.wiley.com). DOI 10.1002/humu.21187

ABSTRACT: Noonan syndrome (NS) and related disorders are autosomal dominant disorders characterized by heart defects, facial dysmorphism, ectodermal abnormalities, and mental retardation. The dysregulation of the RAS/MAPK pathway appears to be a common molecular pathogenesis of these disorders: mutations in *PTPN11*, *KRAS*, and *SOS1* have been identified in patients with NS, those in *KRAS*, *BRAF*, *MAP2K1*, and *MAP2K2* in patients with CFC syndrome, and those in *HRAS* mutations in Costello syndrome patients. Recently, mutations in *RAF1* have been also identified in patients with NS and two patients with LEOPARD (multiple lentigines, electrocardiographic conduction abnormalities, ocular hypertelorism, pulmonary stenosis, abnormal genitalia, retardation of growth, and sensorineural deafness) syndrome. In the current study, we identified eight *RAF1* mutations in 18 of 119 patients with NS and related conditions without mutations in known genes. We summarized clinical manifestations in patients with *RAF1* mutations as well as those in NS patients with *PTPN11*, *SOS1*, or *KRAS* mutations previously reported. Hypertrophic cardiomyopathy and short stature were found to be more frequently observed in patients with *RAF1* mutations. Mutations in *RAF1* were clustered in the conserved region 2 (CR2) domain, which carries an inhibitory phosphorylation site (serine at position 259; S259). Functional studies revealed that the RAF1 mutants located in the CR2 domain resulted in the decreased phosphorylation of S259, and that mutant RAF1 then dissociated from 14-3-3, leading to a partial ERK activation. Our results suggest that the dephosphorylation of S259 is the primary pathogenic mechanism in the activation of RAF1 mutants located in the CR2 domain as well as of downstream ERK.
Hum Mutat 31:284–294, 2010. © 2010 Wiley-Liss, Inc.

KEY WORDS: RAS; MAPK; RAF1; Noonan syndrome; PTPN11; hypertrophic cardiomyopathy

Introduction

Noonan syndrome (NS; MIM# 163950) is an autosomal dominant developmental disorder characterized by facial dysmorphism, including hypertelorism, low-set ears, ptosis, short stature, skeletal abnormalities, and heart defects [Allanson et al., 1985; Mendez and Opitz, 1985]. Frequently observed features in NS patients are pulmonary stenosis (PS), hypertrophic cardiomyopathy, chest deformities, a webbed/short neck, mental

Additional Supporting Information may be found in the online version of this article.

Present address of Yoko Narumi: Department of Medical Genetics, Shinshu University School of Medicine, Matsumoto, Japan.

*Correspondence to: Yoko Aoki, Department of Medical Genetics, Tohoku University School of Medicine, 1-1 Seiryo-machi, Sendai 980-8574, Japan.
E-mail: aokiy@mail.tains.tohoku.ac.jp

retardation, genitourinary defects including cryptorchidism in males, and bleeding diathesis due to factor XI deficiency. The incidence of this syndrome is estimated to be 1 in 1,000–2,500 live births. LEOPARD (multiple *l*entigines, *e*lectrocardiographic conduction abnormalities, *o*cular hypertelorism, *p*ulmonary stenosis, *a*bnormal genitalia, *r*etardation of growth, and sensorineural *d*eafness) syndrome (MIM# 151100) is known to be a NS-related disorder [Digilio et al., 2002]. The features of NS overlap with those of Costello syndrome and cardio-facio-cutaneous (CFC) syndrome. Patients with Costello syndrome (MIM# 218040) show distinctive facial features, mental retardation, high birth weight, neonatal feeding problems, curly hair, nasal papillomata, deep skin creases at palms and soles, and hypertrophic cardiomyopathy [Hennekam, 2003]. CFC syndrome (MIM# 115150) is characterized by distinctive facial features, mental retardation, heart defects (PS, atrial septal defect [ASD], and hypertrophic cardiomyopathy), and ectodermal abnormalities such as sparse, friable hair, hyperkeratotic skin lesions, and a generalized ichthyosis-like condition [Reynolds et al., 1986].

The molecular pathogenesis of these syndromes has been investigated. Tartaglia et al. [2001] have identified missense mutations in *PTPN11*, a gene encoding protein tyrosine phosphatase (PTP) SHP-2, in 45% of clinically diagnosed NS patients. Specific mutations in *PTPN11* has been identified in patients with LEOPARD syndrome [Digilio et al., 2002]. In 2005, we identified *HRAS* germline mutations in patients with Costello syndrome [Aoki et al., 2005]. Mutations in *KRAS*, *BRAF*, and *MAP2K1/2* have been identified in those with CFC syndrome [Niihori et al., 2006; Rodriguez-Viciana et al., 2006]. Mutations in *KRAS* and *SOS1* have also been identified in patients with NS [Roberts et al., 2007; Schubbert et al., 2006; Tartaglia et al., 2007]. Mutations in *NF1* and *SPRED1* have been identified in patients with neurofibromatosis type I (MIM# 162200) [Brems et al., 2007]. These findings suggest that dysregulation of the RAS/RAF/MEK/ERK pathway causes NS and related disorders, and thus it has been suggested that these syndromes be comprehensively termed the RAS/MAPK syndromes [Aoki et al., 2008] or the neuro-cardio-facial-cutaneous syndrome [Bentires-Alj et al., 2006].

In 2007, gain-of-function mutations in *RAF1* were identified in 3–17% of patients with NS and two patients with LEOPARD syndrome [Pandit et al., 2007; Razzaque et al., 2007]. RAF1 is a member of the RAF serine–threonine kinase family and transmits the upstream RAS signaling to downstream MEK and ERK. RAF1, ARAF, and BRAF share three conserved regions, CR1, CR2, and CR3 [Mercer and Pritchard, 2003]. Mutations in *BRAF* identified in patients with CFC syndrome are clustered in CR1 and CR3 domains [Aoki et al., 2008]. In contrast, reported *RAF1* mutations in NS and LEOPARD syndrome were located in the CR2 domain and some mutations were located in CR3 domain. These mutants had enhanced RAF1 kinase activities and most mutations, but not all, showed enhanced phosphorylation of ERK1/2 [Pandit et al., 2007; Razzaque et al., 2007]. Pandit et al. [2007] suggested that RAF1 mutations might interfere with RAF1 phosphorylation at serine 259 as well as with 14-3-3 interaction, and reported that p.P261S did not bind to 14-3-3. However, the mechanisms of RAF1 activation in mutants remain unexplained.

In the present study, we analyzed the *RAF1* gene in 119 patients with NS and related phenotypes without mutations in *PTPN11*, *HRAS*, *KRAS*, *BRAF*, *MAP2K1/2*, and *SOS1*. Detailed clinical manifestations in our new patients with *RAF1* mutations were evaluated, and those in patients with *RAF1 KRAS*, *PTPN11*, and *SOS1* mutations previously reported by us and others were examined. Furthermore, we explored the molecular mechanisms by which RAF1 mutants are activated.

Materials and Methods

Patients

One hundred nineteen patients with NS or related phenotypes were recruited. The primary diagnoses made by clinical dysmorphologists and general pediatricians were as follows: 44 patients with NS, 46 patients with CFC syndrome, 25 patients with Costello syndrome, and 4 patients with atypical phenotypes. No mutations in *PTPN11*, *HRAS*, *KRAS*, *BRAF*, *MAP2K1*, *MAP2K2*, or *SOS1* were identified in these patients. Control DNA was obtained from 105 healthy Japanese individuals. Control DNA from 105 healthy Caucasian individuals was purchased from Coriell Cell Repositories (Camden, NJ). This study was approved by the Ethics Committee of Tohoku University School of Medicine. We obtained informed consent from all subjects involved in the study and specific consent for photographs from six patients.

Mutation Analysis in *RAF1*

Genomic DNA was isolated from the peripheral blood leukocytes of the patients. Each exon with flanking intronic sequences in *RAF1* was amplified with primers based on GenBank sequences (Supp. Table S1; GenBank accession no. NC_000003.10). The M13 reverse or forward sequence was added to the 5′ end of the polymerase chain reaction (PCR) primers for use as a sequencing primer. PCR was performed in 30 μl of a solution containing 10 mM Tris-HCl (pH 8.3), 50 mM KCl, 1.5 mM $MgCl_2$, 0.2 mM dNTP, 10% (v/v) DMSO, 24 pmol of each primer, 100 ng genomic DNA, and 1.5 units of Taq DNA polymerase. The reaction conditions consisted of 35 cycles of denaturation at 94°C for 15 sec, annealing at 55°C for 15 sec, and extension at 72°C for 40 sec. The products were gel-purified and sequenced on an ABI PRISM 310 or 3130 automated DNA sequencer (Applied Biosystems, Foster City, CA).

Determination of the RAF1 Phosphorylation Status

The expression construct, including a *RAF1* cDNA (pUSEamp-*RAF1*), was purchased from Millipore (Billerica, MA). A Myc-tag was introduced at the 5′ terminus of the cDNA by PCR and the PCR product was subcloned into pCR4-TOPO (Invitrogen, Carlsbad, CA). The entire cDNA was verified by sequencing. A single-base substitution resulting in p.H103Q, p.R191I, p.S257L, p.S259F, p.P261A, p.N262K, or p.S427G was introduced using a QuickChange Site-Directed Mutagenesis Kit (Stratagene, La Jolla, CA). All mutant constructs were verified by sequencing. The Myc-tagged wild-type *RAF1* cDNA and mutant cDNAs were digested with *Eco*RI and *Eco*RV and subcloned into the *Eco*RI–*Eco*RV site of the pUSEamp-*RAF1*.

COS7 cells were purchased from the American Type Culture Collection (ATCC, Rockville, MD). Cells were maintained in DMEM containing 10% fetal calf serum (FCS), 50 U/ml penicillin, and 50 μg/ml streptomycin. COS7 cells were seeded at 1×10^5 cells per 6-cm dish, and 24 hr later, 2.0 μg of pUSE vectors encoding one of the wild-type (WT) or mutant RAF1 cDNAs were transfected using 8 μl of PLUS Reagent and 12 μl of Lipofectamine Reagent (Invitrogen). After 3 hr, the medium was replaced to complete medium. After 48-hr culture, cells were scraped and collected by centrifugation after two washes with phosphate-buffered saline

(PBS). Lysates were prepared in 100-μl lysis buffer (10 mM Tris-HCl pH 8.0 and 1% SDS) and boiled for 3 min. The DNA was sheared with a syringe. The lysates were centrifuged at 14,000 × *g* for 15 min at 4°C and protein concentration was determined by Bradford assay. Thirty micrograms of protein was subjected to SDS-polyacrylamide gel electrophoresis (5–20% gradient gel) (ATTO, Tokyo, Japan), transferred to nitrocellulose membrane, and probed with anti-Myc antibody and phospho-specific RAF1 antibodies (Cell Signaling, Danvers, MA). All the membranes were visualized using a Western Lightning ECL-Plus Kit (Perkin-Elmer, Norwalk, CT). The following antibodies were used for Western blotting: anti-Myc (9E10, Santa Cruz Biotech, Santa Cruz, CA), antiphospho-c-Raf (S259) (Cell Signaling), antiphospho-c-Raf (S338) (Millipore), antiphospho-c-Raf (S289/296/301) (Cell Signaling), antiphospho-c-Raf (S621) (Millipore), and antineomycin phosphotransferase II (Millipore).

For immunoprecipitation, lysates were prepared in 1 ml of ice-cold RIPA buffer (50 mM Tris-HCl pH 7.5, 150 mM NaCl, 1 mM EDTA, 1:100 protease inhibitor (Sigma, St. Louis, MO), 1:1000 phosphatase inhibitor (Sigma), and 1% Triton X) and incubated on ice for 15 min. Four hundred micrograms of protein was incubated with anti-Myc (9E10) antibody for 1 hr at 4°C. Immune complexes were collected by adding 50 μl of 50% protein G-Sepharose bead slurry (GE Healthcare, Milwaukee, WI) for 1 hr at 4°C, washed three times with RIPA buffer, and then boiled in 2 × SDS buffer. The samples were resolved in 5–20% gradient polyacrylamide gels, transferred to nitrocellulose membranes and probed with antiphospho-c-Raf (S259) and anti-Myc (9E10) antibodies.

Reporter Assay

NIH 3T3 cells (ATCC) were maintained in DMEM containing 10% newborn calf serum, 50 U/ml penicillin, and 50 μg/ml of streptomycin. One day prior to the transfection, the NIH 3T3 cells were plated in 12-well plates with a density of 1×10^5 cells per well. Cells were transiently transfected using Lipofectamine and PLUS Reagents with 700 ng of pFR-luc, 15 ng of pFA2-Elk1, 7 ng of phRLnull-luc, and 35 ng of WT or mutant expression constructs of *RAF1*. Eighteen hours after transfection, the cells were cultured in DMEM without serum for 24 hr. Cells were harvested in passive lysis buffer, and luciferase activity was assayed using a Dual-Luciferase Reporter Assay System (Promega, Madison, WI). Renilla luciferase expressed by phRLnull-luc was used to normalize the transfection efficiency. The experiments were performed in triplicate. Data are shown as mean ± SD. Statistical analysis was performed using Excel.

Binding of RAF1 with 14-3-3

An expression construct containing Myc- and Flag-tagged 14-3-3 ζ (pCMV6-14-3-3 ζ) was purchased from Origene (Rockville, MD). In order to remove the Myc-tag from the construct, the 3′ half of the cDNA and the Myc-tag were removed by digestion with *Eco*RV and the 3′ half of cDNA was filled using PCR. An S621A mutation, which impairs phosphorylation of S621 to bind 14-3-3, was introduced into pUSE RAF1 harboring WT, p.S257L, or p.N262K cDNA by a Quickchange Site-Directed Mutagenesis Kit. HEK293 cells (ATCC) were transfected with 2 μg RAF1 constructs and 2 μg pCMV6-14-3-3 ζ construct using Lipofectamine and PLUS Reagents. After 48 hr, cells were scraped and collected by centrifugation after two washes with PBS. Lysates were prepared as described above. The Myc-tagged RAF1 was immunoprecipitated with anti-Myc antibody (clone4A6, Millipore) for 1 hr at 4°C. Immune complexes were collected by adding 50 μl of 50% protein G-Sepharose bead slurry (GE Healthcare) for 1 hr at 4°C, washed three times with RIPA buffer, and then boiled in 2 × SDS buffer. The samples were resolved in 5–20% gradient polyacrylamide gels, transferred to nitrocellulose membranes, and probed with anti-FLAG M2 (Sigma) and anti-Myc antibodies. For immunoprecipitation of 14-3-3, anti-FLAG M2 antibody was used and immunoblotting was performed using anti-FLAG M2 and anti-c-Raf (Cell Signaling) antibodies.

Results

Mutation Analysis in Patients

We identified eight amino acid changes in 18 patients (Table 1). A C-to-T nucleotide change, resulting in an amino acid change p.S257L, was identified in 11 patients. Novel p.R191I (c.572G>T) and p.N262K (c.786T>A) were identified in one each patient. Previously reported mutations, including p.S259F (c.776C>T), p.P261A (c.781C>G), p.P261L (c.782C>T), p.S427G (c.1279A>G), and p.L613V (c.1837C>G), were identified in a single patient. Nucleotide numbering reflects cDNA numbering with +1 corresponding to the A of the ATG translation initiation codon in Genbank NM_002880.3, according to journal guidelines (www.hgvs.org/mutnomen). The initiation codon is codon 1. The mutation p.S427G, which has been reported in a patient with therapy-related acute myeloid leukemia [Zebisch et al., 2006], was identified in one patient. None of the newly identified mutations were observed in the control DNA of 105 ethnically matched healthy subjects. Parental samples were obtained from six patients (NS86, 92, 209, 210, 222, and 258). The analysis showed that p.S257L, p.P261A, and p.N262K occurred de novo. p.S427G was also identified as well in his 32-year-old mother, who also exhibited a Noonan phenotype with distinctive facial appearance, sparse hair in infancy, and multiple lentigines. The p.H103Q (c.309C>G) was identified in patient NS86, in whom p.S257L was also identified. This amino acid change was identified in one of his parents without any clinical features, suggesting that this amino acid change was polymorphic.

Clinical Manifestations of Patients with *RAF1* Mutations

Initial diagnoses of patients with *RAF1* mutations were as follows: NS in 11 patients, CFC syndrome in 4 patients, and Costello in 3 patients (Supp. Table S2). Four patients who were first diagnosed as having CFC syndrome were reclassified as NS because of facial features and normal mental development after identification of *RAF1* mutations. Three patients were diagnosed as having Costello syndrome. One patient was rediagnosed as having NS (NS135) and the other patient died at 1 month (NS209). Detailed information on clinical manifestations of NS205 was not available.

Detailed clinical manifestations in 18 patients with *RAF1* mutations were evaluated (Table 2 and Fig. 1). Nine of 15 patients had prenatal abnormality, including cystic hygroma, polyhydramnions, and asphyxia. Most patients had characteristic craniofacial abnormalities frequently observed in NS: relative macrocephaly (94%), hypertelorism (93%), downslanting palpebral fissures (63%), epicanthal folds (86%), and low-set ears (93%). Mental retardation was observed in 6 of 11 (55%) patients. Short stature (73%), short neck (93%), and webbing of neck (81%) were also observed. As for cardiac abnormalities, hypertrophic cardiomyopathy was observed in 10 of 16 patients (63%), followed by pulmonic stenosis (47%),